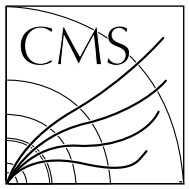

The Compact Muon Solenoid Experiment

CMS Note

Mailing address: CMS CERN, CH-1211 GENEVA 23, Switzerland

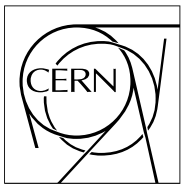

7 June 2006

Study of Flavour Changing Neutral Currents in top quark decays with the CMS detector

C. Karafasoulis, A. Kyriakis, G. Vermisoglou

Institute of Nuclear Physics, NCSR "Demokritos", Athens, Greece

L. Benucci, A. Giammanco[a)], F. Palla

INFN, Pisa, Italy

Abstract

This paper contains the first realistic estimate for the CMS sensitivity to Flavour Changing Neutral Currents (FCNC) in the top quark sector. The non-Standard Model decays $t \to Zq$ and $t \to \gamma q$ (where q represents c or u quarks) have been studied at $\sqrt{s} = 14$ TeV exploiting the leptonic decays of the Z boson and the photon. A realistic detector simulation has been adopted and the most important systematic effects have been addressed. The 5-sigma discovery limits for the two decays are $BR(t \to qZ) = 11.4 \times 10^{-4}$ and $BR(t \to q\gamma) = 5.7 \times 10^{-4}$, allowing some models of new physics to be tested.

[a)] Now at Université Catholique de Louvain,Louvain-la-Neuve, Belgium

1 Introduction

Since the discovery of the top quark at Fermilab [1], top physics has moved from the search phase into the study phase. The top quark is the only known fundamental fermion with a mass at the electroweak scale and, as a result of this large mass, it decays before any hadronisation occurs. This means that studies of the top quark may provide an excellent probe of electroweak symmetry breaking and new physics may well be discovered in either its production or decay. Moreover, predictions for almost all top quark interactions can be evaluated using perturbation theory, thus avoiding uncertainties due to fragmentation processes.

1.1 Top Physics at LHC and new decay channels

As a result of the high instantaneous luminosity and the large $t\bar{t}$ pair production cross-section, the Large Hadron Collider (LHC) will be a 'top factory', producing millions of top events. At hadron colliders $t\bar{t}$ production occurs via QCD-related processes, that is, through the $gg \to t\bar{t}$ or $q\bar{q} \to t\bar{t}$ channels as shown in Figure 1.

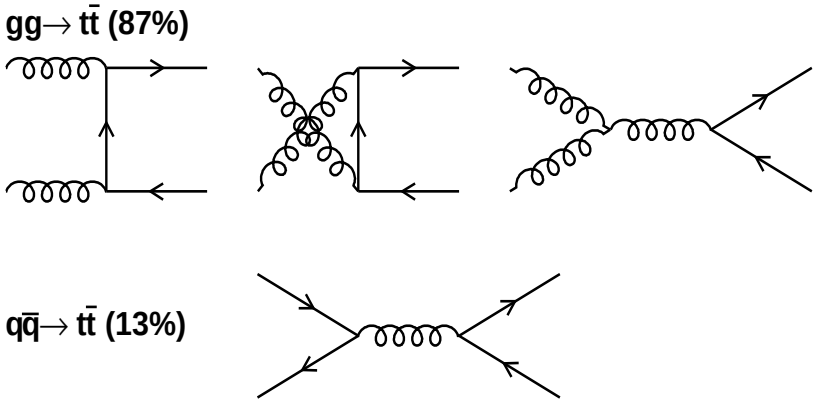

Figure 1: Production of a $t\bar{t}$ pair may occur both via gg fusion and $q\bar{q}$ annihilation. At LHC, the former is expected to be dominant.

At LHC energies ($\sqrt{s} = 14$ TeV), the largest of the proton parton distribution funtions (PDFs) is the gluon density, making $gg \to t\bar{t}$ the principal top production mechanism ($\sim 87\%$). The production cross-section is calculated at $\mathcal{O}(\alpha_s^3)$ and includes the resummation of enhanced leading logarithms. The next-to-leading order (NLO) cross-section prediction (including next-to-leading log (NLL) resummation [2]) is [3]:

$$\sigma(t\bar{t}) = 833 \pm 99\ pb \tag{1}$$

with the error coming from the renormlisation and factorisation scale uncertainties ($\sim 5\%$) and from the PDF uncertainties ($\sim 2.5\%$, [4]). All theoretical results reported here have been evaluated assuming a top mass of 175 GeV/c^2. It is worth emphasizing that this relatively large value for the $t\bar{t}$ cross-section implies that more than 8 million $t\bar{t}$ pairs will be produced per year in low luminosity running at LHC.

In the Standard Model, $t \to bW$ is by far the dominant decay mode ($> 99.9\%$) while other qW decay widths are very small ($BR(t \to sW) \sim 10^{-3}$, $BR(t \to dW) = 10^{-4} \div 10^{-5}$). Equally, the production of such a large amount of top quark pairs at LHC will allow the couplings to both known and new particles to be studied. This may make different decay channels from both the Standard Model and beyond it, accessible for the first time.

1.2 Flavour Changing Neutral Currents in the top sector

Flavour Changing Neutral Current (FCNC) interactions of the top quark involve the anomalous couplings tVc and tVu (where $V = g, \gamma, Z$). The study of these interactions has played an important rôle both in constraining the Standard Model (SM) and in probing possible scenarios for new physics.

Rates for FCNC decays in the top sector are extremely small within the SM [5], due to strong loop suppression and the high masses of the gauge bosons. This makes the top quark significantly different from the other quarks in this respect, and any experimental evidence for a top quark FCNC interaction would be an indication of new physics.

In recent years, a wide range of studies have been made of anomalous top quark couplings. On the theoretical side, both FCNC top quark decays and top-charm associated production at high energy colliders have been extensively studied both in the SM [6] and in models beyond it, such as the two Higgs doublet models (2HDM), the Minimal Supersymmetric Standard Model (MSSM) ([7] - [10]) (where the introduction of broken R-parity models could give rise to large cross-section enhancements) and other exotic extra-quark models [11]. In these new physics scenarios the top quark FCNC branching ratios may rise to the values reported in Table. 1. On the experimental side, current limits on top quark FCNC branching ratios have been derived from low-energy data, direct searches of rare top decays at the Tevatron, deviations from the SM predictions for $t\bar{t}$ production and searches for single top production at LEP2 and HERA. Currently, the most stringent limits are those given in the last column of Table. 1. They come from the ZEUS experiment (single top production via FCNC in $e^{\pm}p \rightarrow e^{\pm}p(t/\bar{t}) + X$, [12]), LEP2 ($e^+e^- \rightarrow \bar{t}c$ or $\bar{t}u$, [13]) and the CDF experiment ($t\bar{t}$ pair production cross-section, including the theoretical assumptions reported in [14]).

Table 1: Branching ratio predictions for FCNC top quark decays from the SM and from four SM extensions, with the corresponding current experimental limits.

	SM	2HDM	SUSY	SUSY with $\not{R}$	Exotic quarks	Exp. Limits (95% CL)
BR($t \rightarrow qg$)	5×10^{-11}	$\sim 10^{-5}$	$\sim 10^{-6}$	$\sim 10^{-3}$	$\sim 5 \times 10^{-4}$	0.29 (CDF)
BR($t \rightarrow q\gamma$)	5×10^{-13}	$\sim 10^{-7}$	$\sim 10^{-8}$	$\sim 10^{-5}$	$\sim 10^{-5}$	0.0059 (ZEUS)
BR($t \rightarrow qZ$)	$\sim 10^{-13}$	$\sim 10^{-6}$	$\sim 10^{-8}$	$\sim 10^{-4}$	$\sim 10^{-2}$	0.14 (LEP2)

This work contains an estimation of the observability of the non-SM signals $t \rightarrow Zq$ and $t \rightarrow \gamma q$ with the CMS experiment, that is, studied using the full detector simulation and the official reconstruction software packages.

First the topology and features of both the signal and the relevant backgrounds are presented, followed by parton-level studies devised to find the most appropriate strategy for signal reconstruction. This strategy is subsequently applied to samples of fully simulated data and limits on the branching ratios for both $t \rightarrow Zq$ and $t \rightarrow \gamma q$ in a low-luminosity scenario are evaluated. The impact of systematic uncertainties on the measured sensitivity is then presented, followed by conclusions and the outlook for this analysis.

2 Signal simulation and relevant background sources

All the signal samples are generated assuming pp collisions at a centre-of-mass energy of $\sqrt{s} = 14$ TeV, adopting the following values for the relevant masses: $M_Z = 91.1876$ GeV/c^2, $M_W = 80.22$ GeV/c^2, $m_t = 175$ GeV/c^2. The FCNC signal samples were generated using the specialised event generator TopReX 4.11 [15] while PYTHIAversion 6.227 [16] was used for both hadronisation and fragmentation. The CTEQ5L PDF set was used, assuming a hard scale of $Q^2 = m_t^2$. Initial and final state QED and QCD (ISR, FSR) radiation have been included, along with underlying events and multi-parton interactions.

The signal presented here is made up of a $t\bar{t}$ pair, where one of the top quarks decays via the SM process, $t \to W^+b$ ($\bar{t} \to W^-\bar{b}$) and the other decays through the FCNC process, $\bar{t} \to V\bar{q}$ ($t \to Vq$), where $V = \gamma, Z^0$ and $q = u, c$. Given the current upper limits for the FCNC branching ratios (Table. 1), it is reasonable to assume that the contribution from events in which both top quarks decay via a FCNC process can be ignored. Only the leptonic decays have been considered both for the Z^0 ($Z^0 \to ll$) and for the $W^\pm$ ($W \to l\nu$), where l indicates an electron or muon and ν an electron or muon neutrino (Figure 2). Hadronic decays and τ decays have not been considered, because they are significantly harder to identify and are affected by a very large multi-jet QCD background. In spite of the small branching ratios, especially in the qZ case ($BR(Z \to ll) = 0.06715$, $BR(W \to l\nu) = 0.2161$), this signal is expected to have a very distinctive experimental signature. The generated signal sample is a mixture of the two charge-conjugated final states $t\bar{t} \to (Vq)(Wb)$ and $t\bar{t} \to (Wb)(Vq)$ and amounts to 8000 events each for the $V = Z^0$ and $V = \gamma$ channels.

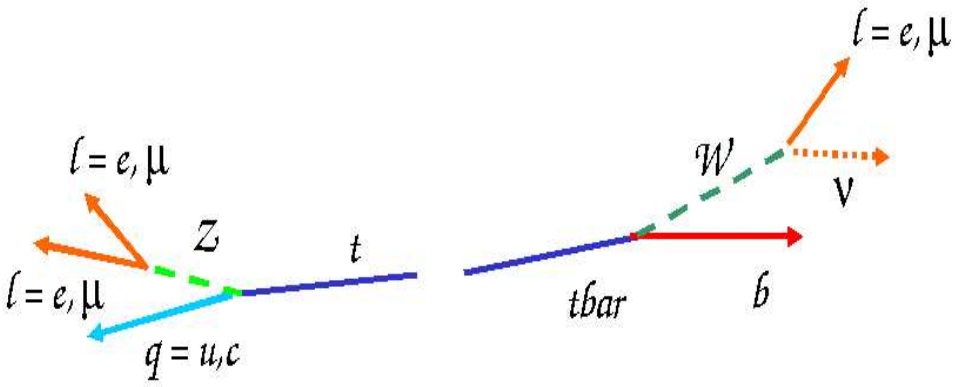

Figure 2: An example of the event topology in which one top quark decays to Zq, while the other decays to Wb. The same event topologies are considered for the $t \to \gamma q$ case.

The generated events are passed through the full detector simulation [17] and digitization chain [18], assuming a low luminosity scenario with $\mathcal{L} = 2 \times 10^{33} cm^{-2} s^{-1}$. The only exceptions are two of the event samples used in the $t \to \gamma q$ analysis, which are instead passed through the fast simulation and reconstruction package [19].

2.1 Backgrounds for the $t \to Zq$ channel

The most distinctive features of the $t \to Zq$ channel are the presence of large missing energy and three leptons with high transverse momentum (the decay products of the W and Z bosons). In addition, the events must contain two hard jets coming from the fragmentation of the b from the SM top decay and the light quark from the FCNC top decay, respectively. It is natural to first identify the SM top decay by looking at the invariant mass distribution of the reconstructed W combined with a jet initiated by a b quark (b-jet). The FCNC top decay should then appear as an excess in the $M(qZ)$ invariant mass distribution, recoiling in a direction (in the transverse plane) opposite to the other top quark.

In principle, all the processes which could produce three hard isolated leptons have to be taken into account as sources of background, as the leptons could mix with hard jets coming from flavour excitations, initial/final state QCD radiation or gluon splitting. At LHC energies, such processes have relatively large cross-sections and could therefore create significant background in the $M(qZ)$ distribution, making it harder to identify real FCNC top decays.

The background sources which have been considered are listed below, while the corresponding cross-sections are reported in Table. 2:

- *multi-jet production*: In the high-multiplicity LHC environment, QCD is one of the most challenging backgrounds for many analyses. Many jets initiated by light quarks (light-quark jets) will be produced, but the requirement of three hard isolated leptons in any given event strongly suppresses the contribution from this background source. It appears that multi-jet QCD events will be completely rejected from this analysis, so they are not considered further;

- *$t\bar{t}$ production*: When both top quarks decay via the SM decay channel, it is possible to produce two hard isolated leptons from the decay of the two W bosons. In this case, one of the top quarks will be reconstructed correctly, while the other may "fake" a FCNC decay if the identification of the b-jet fails. For other possible W decay channels, the rate of production of three hard isolated leptons is much lower and therefore only the case where both W bosons decay leptonically is considered here. As these events are also initiated by $t\bar{t}$ production, this source of background is considered to be the most important;

- *Di-boson production*: Events in which either a ZZ, ZW or WW pair is produced are natural candidates to pass the W and Z selection, if they decay leptonically. However, the additional requirement of the presence of a b-jet strongly suppresses the contribution from this background source. Moreover, the cross-section for WZ and ZZ production are quite small;

- *Z or W plus jets production*: These background sources include processes such as $q\bar{q} \rightarrow Zg$, $qg \rightarrow Z/Wq$ and $q\bar{q}' \rightarrow Wg$ which, by picking up additional leptons, could pass the qZ or bW selection requirements, particularly as the cross-section for this set of processes is expected to be large. These background sources are best suppressed by ensuring good b-jet identification and applying invariant mass constraints. The cross-section both for Z plus jets and W plus jets increases dramatically with decreasing $\hat{p}_T$ of the outgoing parton, indicating that the sensitivity of the analysis to these background sources will depend on this hard scale. As will be seen later, only events in the range 40$< \hat{p}_T <$300 GeV/c are expected to have a sizeable effect;

- *Boson production in association with a $b\bar{b}$ pair*: Even at large values of $\hat{p}_T$ the cross-sections for these processes remain high. If the b-jet identification fails, such events can easily fake both the SM and FCNC top decays. It is expected that good lepton isolation requirements (in order to reject leptons from semi-leptonic b decays) and invariant mass requirements will be very effective in reducing the $W \rightarrow l + b\bar{b}$ contribution, but the rejection of $Z \rightarrow 2l + b\bar{b}$ events is much more problematic. In order to estimate this source of background, a sample of Drell-Yan events ($(\mu^+\mu^-) + b\bar{b}$, with $M(\mu^+\mu^-) > 5$ GeV/c) is used, in which the majority of these events are actually the result of an off-shell photon splitting into a $\mu^+\mu^-$ pair;

- *Single top production, $t \rightarrow l + X$*: Single top events, in which the top quark is produced in association with a W boson or a light quark, could pass both the SM and the FCNC top decay selection requirements, as each event contains a real top quark and only one b-jet. However, it is expected that the requirement of three hard isolated leptons will heavily suppress this source of background and it is therefore assumed to be negligible.

2.2 Backgrounds for the $t \rightarrow \gamma q$ channel

Events containing a $t \rightarrow \gamma q$ decay can be identified by looking for a high-energy isolated photon in association with a top quark decaying via the SM decay channel. This means that the events must contain one b-jet and one light-quark jet in order to separate them from SM $t\bar{t}$ events. The sources of background considered for this decay channel are listed below and their cross-sections are reported in Table. 3:

- *multi-jet production*: QCD background has a much more severe impact in this case compared to the $t \rightarrow Zq$ channel, because a large number of photons are normally produced inside jets. The

Table 2: The cross-sections, expected number of events for an integrated luminosity of L=10 fb^{-1} and the size of the event samples for the different sources of background considered for the $t\bar{t} \to (Wb)(Zq)$ decay channel. The symbol l denotes the sum of the μ, e and τ contributions.

Background process	$\sigma \times Br(pb)$	Events (L=10 fb^{-1})	Events Analysed
$t\bar{t} \to (bW)(bW) \to (bl\nu)(bl\nu)$	85	850K	908K
$WW + X \to (l\nu)(l\nu) + X$	19.8	198K	93K
$WZ + X \to (l\nu)(ll) + X$	2.6	26K	49K
$ZZ + X \to (ll)(ll) + X$	0.16	1.6K	93K
$Z(\to ll) + jets$ (40< $\hat{p}_T$ <300)GeV/c	576.4	5764K	191K
$Z(\to \mu\mu) + b\bar{b}$	116	1160K	98K

cross-section for this process decreases rapidly with the $\hat{p}_T$ of the outgoing parton, which means that the sensitivity of this analysis to this background source depends on the hard scale. For this reason a number of event samples covering the range $50 < \hat{p}_T < 1000$ GeV/c have been studied;

- *$t\bar{t}$ production*: In this case the top quark which decays via the SM decay channel will be identified correctly, while the other top quark can mimic the FCNC top decay if an electron is misidentified as the photon or if a photon is produced in the decay of a π^0. This process has a large cross-section, making it the most important source of background for this analysis. It has been explicitly ensured that all $t\bar{t}$ processes in which a photon is found in the final state along with two hard isolated leptons have been included in this sample;

- *Di-boson production*: Events in which a ZZ, ZW or WW pair is produced are a particularly important background not only from the W boson reconstruction point of view, but also as a source of light-quark jets and fake photons. As in the $t \to Zq$ case, these processes can imitate both the SM top decay and the FCNC top decay if the b-jet identification procedure fails. The contribution from events containing a ZZ pair are the least important, as the cross-section is very small and they tend to fail the missing energy requirement;

- *Z or W plus jets production*: As in the $t \to Zq$ channel, these processes can easily mimic the signal process, particularly if the b-tagging procedure fails. The cross-section for these background processes is very large, so they must be considered an important source of background. These events are most effectively rejected by requiring a strong recoil between the two top quarks. Once again, this process depends strongly on the $\hat{p}_T$ of the outgoing parton, but it has been observed that only events in the range $80 < \hat{p}_T < 150$ GeV/c make a significant contribution;

- *Boson production in association with a $b\bar{b}$ pair*: As the cross-sections for these processes are large, it is expected that this will be an important source of background. However, it is expected that the missing energy requirement will easily reject events in which a Z boson is produced and so these processes are not considered further;

- *Boson plus photon production*: The production of events containing either a W or a Z in association with a hard isolated photon should also, in principle, be considered. However, the cross-sections for such processes are extremely low and should be completely rejected by the requirement of one b-jet per event. On this basis, this background contribution was neglected;

- *Single top production, $t \to l + X$*: As for the $t \to qZ$ channel, single top events may be a source of background if the particles produced in association with the top quark could be misidentified as a $t \to q\gamma$ decay. On the assumption that the probability of these events containing a fake photon candidate is similar, regardless of the single top production channel, only the s-channel is considered here because it has the largest cross-section.

Generally speaking, single top production should play an important rôle in such analyses, as FCNC decays have exactly the same probability to appear, even if only one top quark is produced. However,

Table 3: The cross-sections, expected numbers of events for an integrated luminosity of L=10 fb^{-1} and the size of the event samples for the different sources of background considered for the $t\bar{t} \to (Wb)(\gamma q)$ channel. The symbol l denotes the sum of the μ, e and τ contributions.

Background process	$\sigma \times Br(pb)$	Events (L=10 fb^{-1})	Events Analysed
QCD (50< $\hat{p}_T$ <80)GeV/c	20917910	209179M	92K
QCD (80< $\hat{p}_T$ <120)GeV/c	2946763	29467M	96K
QCD (120< $\hat{p}_T$ <170)GeV/c	499156	4991M	93K
QCD (170< $\hat{p}_T$ <230)GeV/c	100800	1008M	93K
QCD (230< $\hat{p}_T$ <300)GeV/c	24470	225M	93K
QCD (300< $\hat{p}_T$ <380)GeV/c	6384	64M	93K
QCD (380< $\hat{p}_T$ <470)GeV/c	1887	19M	96K
QCD (470< $\hat{p}_T$ <600)GeV/c	683	6.8M	96K
QCD (600< $\hat{p}_T$ <800)GeV/c	204	2.0M	90K
QCD (800< $\hat{p}_T$ <1000)GeV/c	35.1	351K	80K
$t\bar{t}$ *inclusive*	833	8330K	780K
$WW + X \to (l\nu)(l\nu) + X$	19.8	198K	93K
$WZ + X \to (l\nu)(ll) + X$	2.6	26K	49K
$W(\to l\nu) + jets$ (80< $\hat{p}_T$ <150)GeV/c	4302.6	43026K	186K
$W(\to l\nu) + bb$	300	3000K	126K
$t + q \to (bW) + q \to (bl\nu) + q$	81.2	812K	384K

as this analysis explicitly requires the presence of two top quarks, one of which must decay via the SM decay channel, the selection efficiency for identifying single top events in which the top decays via the FCNC decay channel should be very low and therefore single top processes are only considered as a source of background.

3 The FCNC $t \to Zq$ decay channel analysis

When searching for a $t \to Zq$ signal, two major issues must be considered: The selection of the three leptons coming from W and Z decays and the discrimination between the light-quark and the b-jets. A strategy for addressing these issues, while ensuring high efficiency and low background contamination is outlined below.

3.1 Parton-level studies

A study of the distributions of the different kinematic variables associated with signal events has been performed at the parton level. In Figures 3 and 4 the p_T and η distributions of the Z, W and b quark are shown, along with the same distributions for the leptonic decay products. It can be seen that the Z and the W are centrally produced. The p_T distributions of the Z and W should be very similar to the outgoing parton, as they will be produced in a "back-to-back" configuration. This therefore explains why, for some $\hat{p}_T$ dependent background processes, only a certain range in $\hat{p}_T$ is important.

3.2 Signal reconstruction procedure

As only events in which the W and Z bosons decay leptonically are considered in this analysis, the "double electron or double muon" trigger criteria can be employed to select events at Level 1 (L1) and in the High Level Trigger (HLT). In the HLT, isolated leptons are only considered if they have passed the following trigger thresholds: In the case of the di-muon trigger, both muons must satisfy $p_T > 7$ GeV/c, while in the di-electron case, the requirement is $p_T > 17$ GeV/c. For single muons the threshold is $p_T > 19$ GeV/c and for single electrons the threshold is $p_T > 29$ GeV/c. Full details may be found

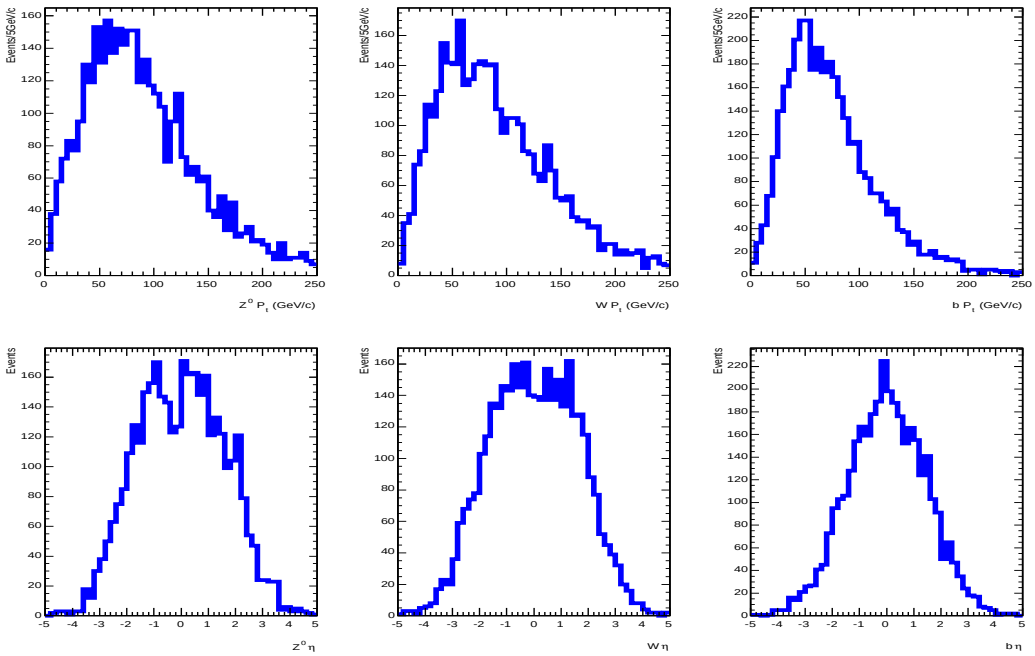

Figure 3: Distributions of kinematic variables for key particles in $t\bar{t} \to (Zq)(Wb)$ events. The upper plots show the p_T distributions of the Z (left), W (centre) and b quark (right), while the bottom plots show their corresponding η distributions. The signal samples are a equal mixture of $t\bar{t} \to (Zq)(W\bar{b})$ and $t\bar{t} \to (Wb)(Z\bar{q})$ events.

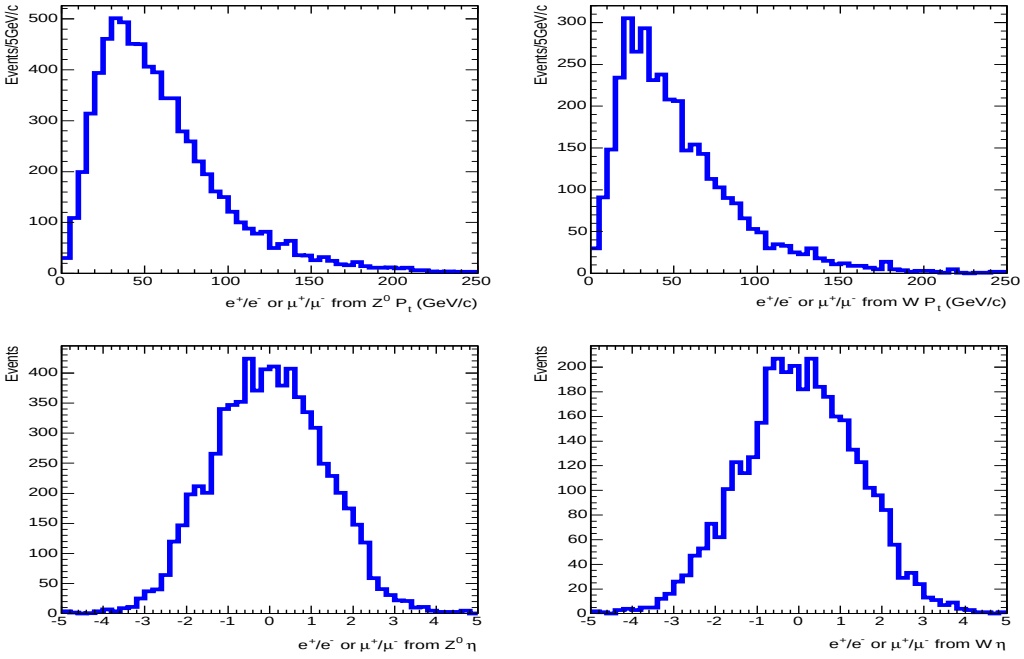

Figure 4: Distributions of kinematic variables for key final state particles in the $t\bar{t} \to (Zq)(Wb)$ decay. The upper plots show (from left to right) the p_T distributions of the electron and muon coming from the Z decay and the electron and muon coming from the leptonic W decay, while the bottom plots show their correspoinding η distributions.

in [20]. In this analysis, the double-lepton trigger is exploited, with high signal acceptance efficiencies: 90% at L1 and 89% in the HLT.

3.2.1 Lepton reconstruction and identification

Offline, events are initially selected by requiring the presence of three leptons, missing transverse energy, exactly one b-jet and one light-quark jet. The leptons are only accepted if they satisfy $p_T > 10/20$ GeV/c for muons/electrons respectively. Additional selection requirements (offline quality cuts) must be applied in order to reject misidentified leptons or leptons from decays other than those of the Z and W bosons. The standard CMS selection scheme [21] has been employed in this analysis and is briefly summarised below. All tracks used in this analysis have been reconstructed using a combination of the Pixel detector and the Silicon Strip Tracker.

- The energy deposits from an electron will tend to be fully contained within the electromagnetic calorimeter (ECAL), while low p_T hadrons ($p_T > 20 \div 30$ GeV/c) tend to also deposit energy in the hadron calorimeter (HCAL). A requirement that the electron candidate satisfies $E_{HCAL}/E_{ECAL} < 0.03$ is therefore made;
- When considering electron candidates, the energy in the calorimeter is required to closely match the corresponding track momentum by accepting only candidates which satisfy $E(e)/p_T(e) > 0.8$;
- Lepton candidates are only considered if they are isolated. A candidate is considered to be isolated if it satisfies the following criteria: A cone of radius $\Delta R = \sqrt{(\Delta\eta)^2 + (\Delta\phi)^2} = 0.3$ is defined around the candidate lepton track. The p_T of all good tracks not associated to the lepton, but which lie within this cone are then summed. A good track is defined as one which satisfies $p_T >$ 0.9 GeV/c and has more than four hits in the tracking detectors associated to it. If this p_T sum is less than 4% of the $p_T(E_T)$ of the muon(electron) candidate, respectively, then the candidate lepton is considered to be isolated. To attain the strongest isolation requirements, no matching in transverse plane and in longitudinal direction between the lepton track and the tracks inside the cone is applied,since if the lepton comes from semileptonic b-quark decays this matching condition is rather poor;
- When considering electron candidates, if multiple tracks point to the same electromagnetic cluster, the best track is assumed to be that closest in η to the cluster, where the η separation is defined as that between the centre of the electromagnetic cluster within the ECAL and the track position when extrapolated to the ECAL face.

Figures 5 and 6 show the p_T distributions for electron and muon candidates after the application of both trigger and offline quality cuts in both the signal events and in the different background samples. In addition, the corresponding distributions for "matched" lepton candidates are shown, ie. those candidates which have been found to lie within a cone of radius $\Delta R = 0.3$ around the true particle direction from the generator-level. The comparison of these distributions demonstrates whether the selection procedure is working correctly. In this case, it can be seen that the distributions are very similar, particularly at high p_T.

3.2.2 Jet identification and missing energy reconstruction

All jets are reconstructed using an iterative cone algorithm with a radius of $\Delta R < 0.5$, which is run over transverse energy deposits in the CMS calorimeters ($\vec{E}_T(tower)$). The calibrated jet energies $\vec{E}_T^{calib}(jet)$ are then determined based on the "raw" jet energies ($\vec{E}_T^{raw}(jet)$) using the "gamma-jet" method [23].

The missing transverse energy is then calculated using the expression:

$$\vec{\not{E}}_{\mathrm{T}} = -\sum \vec{E}_T(tower) - \sum \left(\vec{E}_T^{calib}(jet) - \vec{E}_T^{raw}(jet)\right) \quad (2)$$

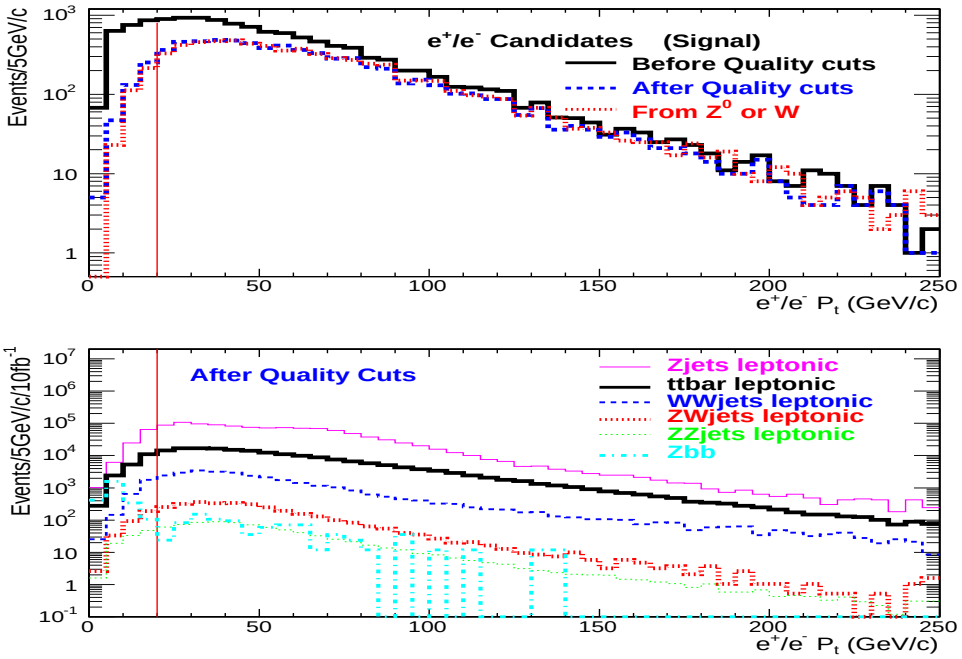

Figure 5: The transverse momentum distributions of $e^{\pm}$ candidates after trigger requirements in both the signal sample and the different background samples. The line indicates the offline p_T requirement ($p_T > 20$ GeV/c). The corresponding distributions after the quality cuts have been applied are also shown. The background samples have been normalised to reflect an integrated luminosity of L=10 fb $^{-1}$.

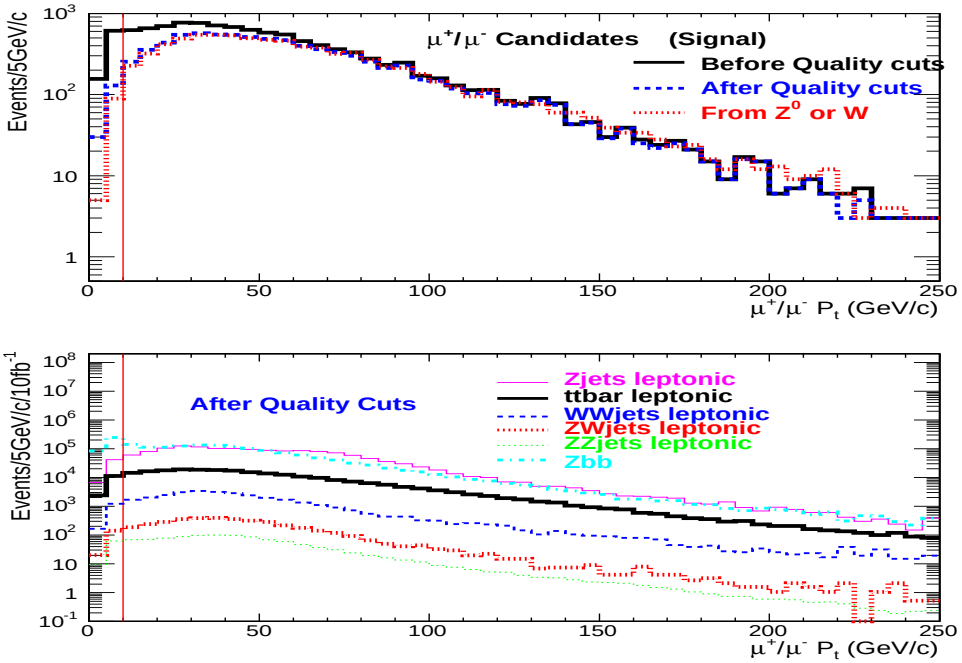

Figure 6: The transverse momentum distributions of $\mu^{\pm}$ candidates after trigger requirements in both the signal sample and the different background samples.The line indicates the offline p_T requirement ($p_T > 10$ GeV/c). The corresponding distributions after the quality cuts have been applied are also shown. The background samples have been normalised to reflect an integrated luminosity of L=10 fb $^{-1}$.

where raw jets are only used if $\vec{E}_T^{raw}(jet) > 10$ GeV. This method was found to give the distribution closest to the p_T distribution of the neutrinos from the decay of the W. The distribution of missing transverse energy is shown in Figure **??**. The small differences between the two distributions in the top of Figure **??** have been ascribed to detector effects and the products of semileptonic heavy quark decays.

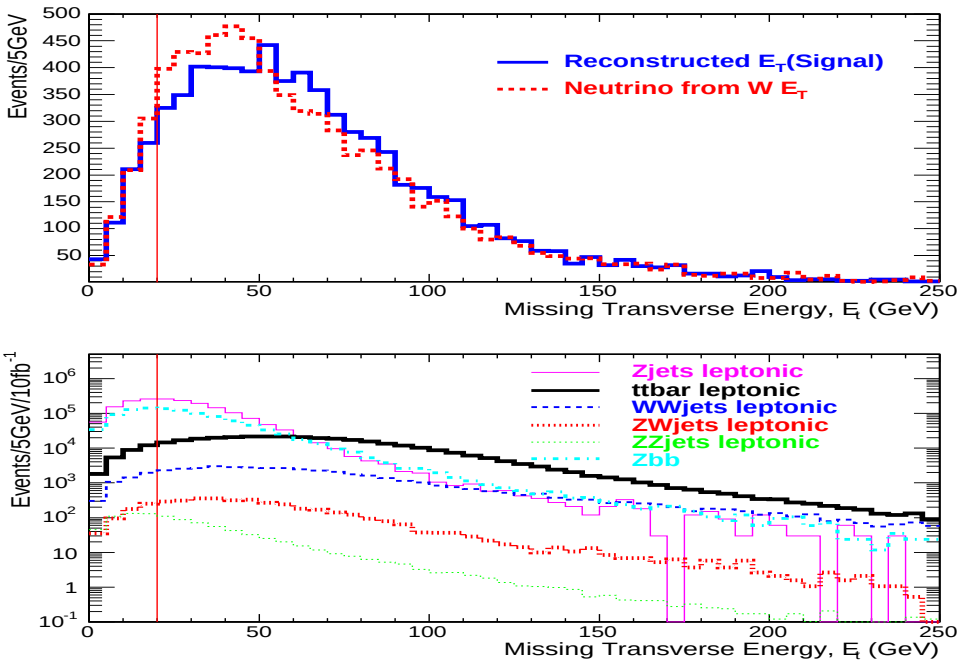

Figure 7: The distribution of missing transverse energy in both the signal sample and the different background samples. The line indicates the offline requirement of $E_T > 20$ GeV. The agreement between the measured missing transverse energy and that from the generator-level neutrinos from the decay of the W is reasonable.

3.2.3 Selection of b-jets and light-quark jets

Good b-jet identification is crucial for this analysis, as the requirement that every event contains at least one b-jet is very effective in the suppression of all non-top sources of background, while the requirement of no more than one b-jet is effective in reducing the contribution from the SM $t\bar{t}$ background. The "combined b-tagging" algorithm [24] is applied to calibrated iterative cone jets to make the b-jet selection. Figure 8 shows the distribution of the discriminator value produced by this algorithm for both b-jets and charm jets. The criteria for identifying jets which are highly likely to come from a b quark ("b-tagged" jets), are that the jet must contain at least two tracks and have a discriminator value greater than 1.5. This suppresses the contribution from charm-jets.

Jets which have passed the b-tagging requirements are only accepted for further analysis if they also satisfy p_T >40 GeV/c. The transverse momentum distribution of these jets is shown in Figure 9. It can clearly be seen in the figure that the correct identification of the b-jet from the top decay is much less likely for low values of p_T due to the increased hadronic background and reduced b-tagging efficiency in this region. At higher values of p_T, the purity of the b-jet selection is above 90%.

The use of this algorithm results in a b-tagging efficiency of about 30%: Based on previous studies of b-tagging in a multi-jet QCD MC sample [24], this implies that charm jets will be mis-tagged in about 0.9% of cases, uds-jets will be mis-tagged $1 \div 5 \times 10^{-4}$ of the time and gluon-initiated jets will be mis-tagged in about 0.5% of cases. This means that the dominant contribution to the mis-tagging rate is from gluon-initiated jets, as they constitute approximately 70% of the QCD multi-jet background sample and hence 0.5% is taken as the upper limit on the mis-tagging rate for this algorithm. It is worth noting that this is a conservative estimate as the gluons will predominantly split into light quarks.

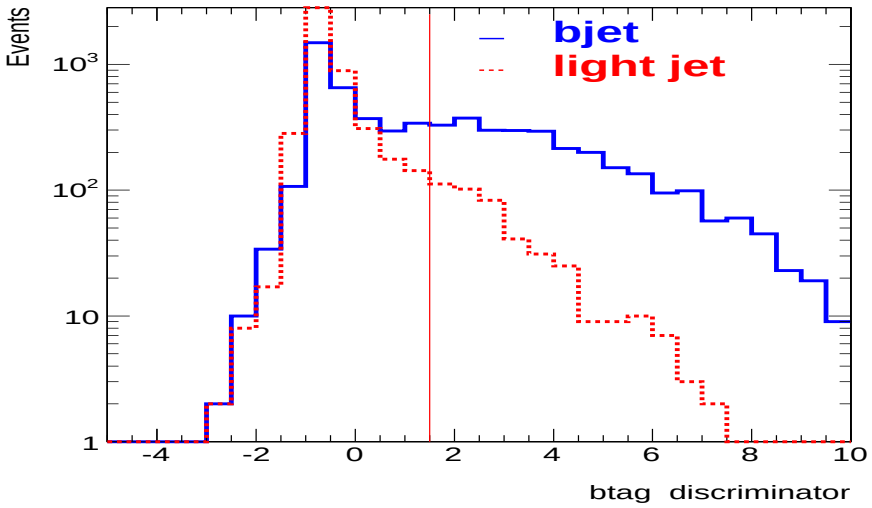

Figure 8: The distribution of the discriminator variable output by the "combined b-tagging" algorithm (see text for full details) for charm-tagged jets and for b-tagged jets, as determined from generator-level MC information. The vertical line shows the cut value (> 1.5) chosen in the Zq analysis to suppress the contribution from charm-jets.

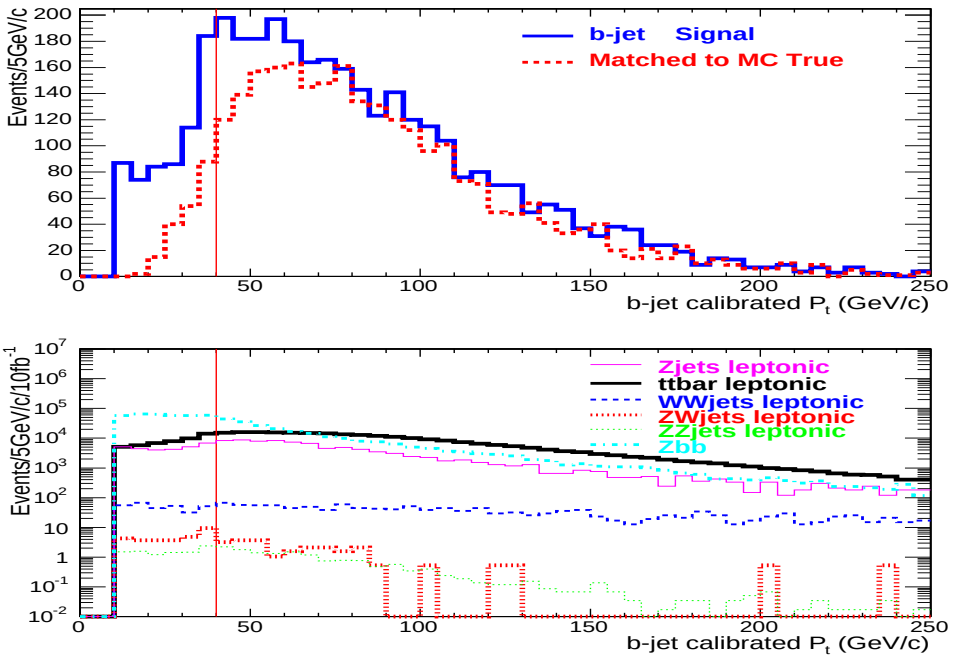

Figure 9: The distribution of the transverse momentum of b-jet candidates in the signal sample and in the different background samples. The line indicates the offline p_T requirement applied to the jets ($p_T > 40$ GeV/c). The corresponding distribution for jets matched to the generator-level b quark from the SM top decay is also shown. The background distributions have been normalised assuming an integrated luminosity of L=10 fb^{-1}.

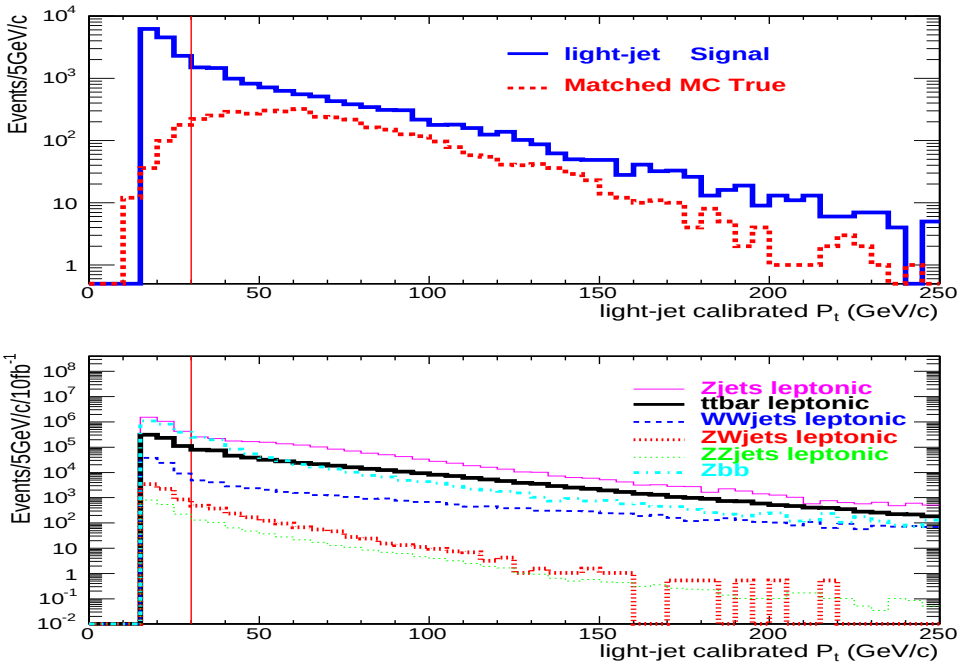

Figure 10: The distribution of the transverse momentum of light-quark jet candidates in the signal sample and in the different background samples. The line indicates the offline p_T requirement applied to the jets ($p_T > 30$ GeV/c). The corresponding distribution for jets matched to the generator-level light quarks from the FCNC top decay is also shown.

All jets which fail the b-tagging requirements are assumed to be light-quark jet candidates. Of these remaining jets, only those which are well-separated from the b-tagged jet ($\Delta R > 0.02$), do not include an electron cluster and have an $\eta < 2.3$ are retained. A minimum transverse momentum requirement of $p_T >$30 GeV/c is also made. As shown in Figure 10 the comparison of the light-quark jet p_T distribution with that from the matched jets demonstrates that it is difficult to correctly identify the light-quark jet from the FCNC top decay, as additional jets from higher-order QCD processes constitute an abundant source of fake jets. These can only be rejected by requiring the presence of all the other expected final state objects, whose reconstruction is described in the following sections.

3.2.4 Constraints on the Z^0 mass

In the case of the $t \to qZ^0$ channel, the Z^0 is reconstructed by combining two same-type, but opposite-sign leptons. The pair of leptons in each event whose invariant mass lies closest to that of the Z^0 is assumed to be correct one. This selection criterium is very effective in selecting the correct Z^0 candidate, although it also leads to a background distribution with a maximum in the region around the Z^0 peak. However, it can also be seen in the invariant mass distribution in Figure 11 that the contribution from combinatorial background is only a fraction of the size of the signal peak.

The invariant mass distribution shows the expected asymmetry on the low side of the peak, which is caused by photon radiation. Clearly, the most dominant source of background for this distribution comes from the Z^0 plus jets sample, particularly given the large cross-section for this process. In order to exclude lepton-pairs which do not come from a Z^0 decay effectively, a narrow mass window around the Z^0 peak is chosen. In this analysis, the lepton pair is only kept if its invariant mass satisfies $|M(ll) - M_Z| < 10$ GeV/c^2. Events with more than one good Z^0 candidate are rejected.

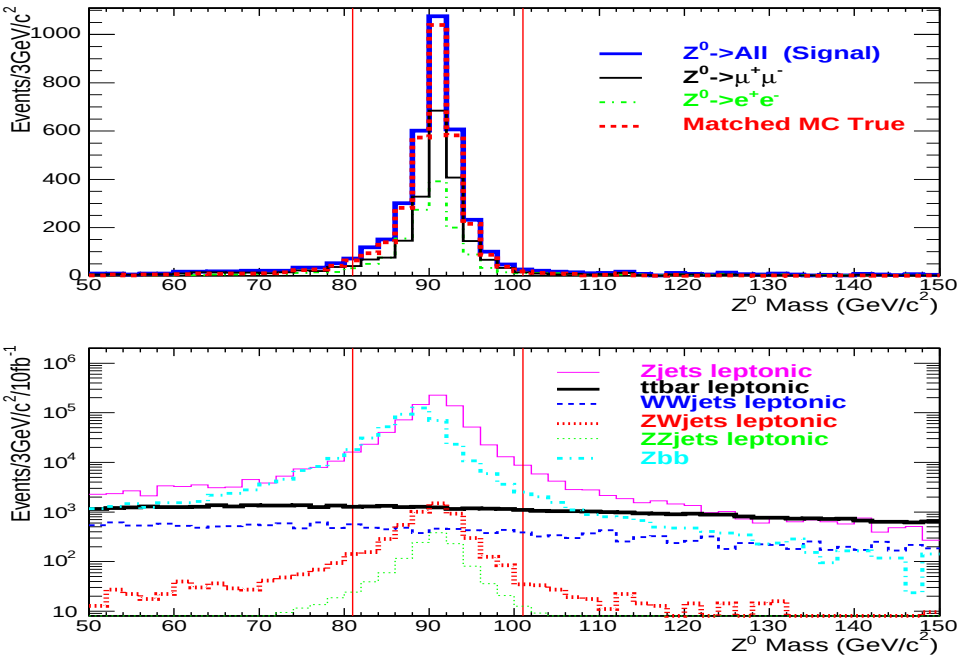

Figure 11: The e^+e^- and $\mu^+\mu^-$ invariant mass distributions in the signal sample and in the different background samples. The lines indicate the window in which lepton-pairs are accepted as good Z^0 candidates. The background distributions are normalised assuming an integrated luminosity of L=10 fb^{-1}.

3.2.5 Constraints on the $W^{\pm}$ mass

The search for a W boson in candidate events is constrained by requiring that the event should already contain a good Z^0 candidate. This is very effective in rejecting events which contain less than three hard leptons (the WW, Z plus jets and $t\bar{t}$ background samples). The lepton from the decay of the W boson must satisfy $p_T > 15$ GeV/c and the missing transverse energy in the event must be greater than 20 GeV, to reject events in which a neutrino is produced, but not in the decay of the W boson. The transverse mass of the lepton-$\not{E}_{\rm T}$ combination is then calculated from:

$$M(l\ \not{E}_{\rm T})_T = \sqrt{(p_T(l) + \not{E}_{\rm T})^2 - (p_x(l) + p_x(\nu))^2 - (p_y(l) + p_y(\nu))^2} \qquad (3)$$

The distribution of the transverse mass is shown in Figure 12 and clearly exhibits the typical Jacobian shape, smeared by the finite detector energy resolution. In each event, the lepton-missing transverse energy combination with the invariant mass closest to the mass of the $W^{\pm}$ is kept, provided it satisfies $M(l\ \not{E}_{\rm T})_T$ <120 GeV/c^2. Any event containing more than one good W candidate is rejected.

3.2.6 Constraints on the mass of the top candidate from the SM decay channel

The contribution from the inclusive $t\bar{t}$ background sample can be further suppressed by requiring that each candidate event contains only one b-jet. That b-jet must be combined with the reconstructed W candidate in order to determine the mass of the top quark that produced them. In order to do this, the longitudinal component of the missing energy vector, $p_z(\nu)$, must be determined. This is done by solving the following quadratic equation:

$$M_W^2 = 2\left(E(l)\sqrt{p_z^2(\nu) + \not{E}_{\rm T}^2} - p_x(l)p_x(\nu) - p_y(l)p_y(\nu) - p_z(l)p_z(\nu)\right)$$

This equation has two solutions:

$$p_z^{1,2}(\nu) = \frac{Ap_z(l) \pm \sqrt{\Delta}}{p_T(l)^2}$$

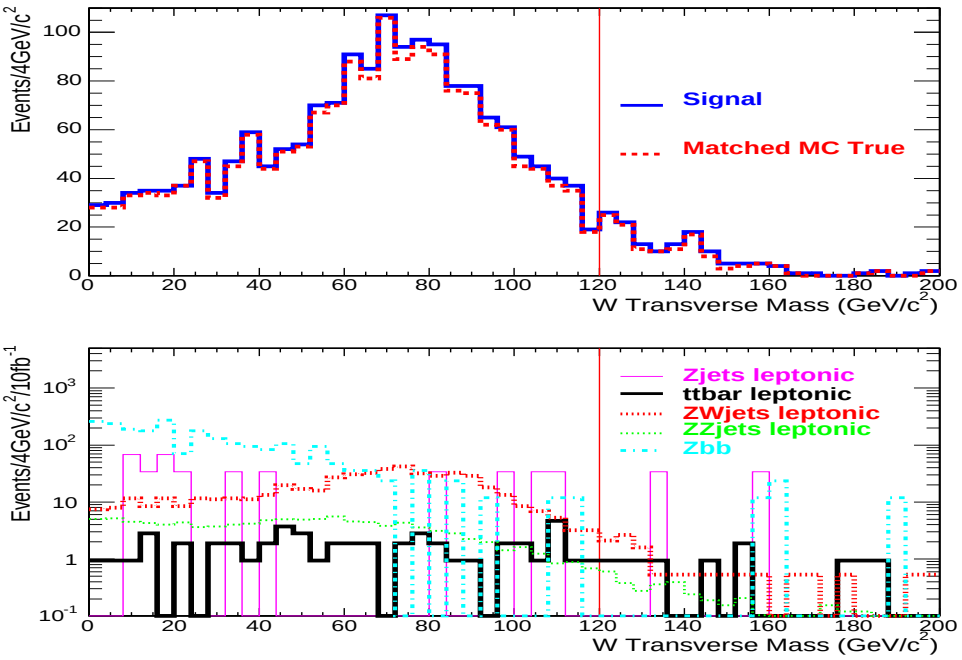

Figure 12: The distribution of the tranverse invariant mass of the $e^{\pm}$ or $\mu^{\pm}$-missing energy combination in the signal sample and in the different background samples. The line indicates the accepted mass region($< 120 GeV/c^2$). The background distributions have been normalised assuming an integrated luminosity of L=10 fb^{-1}.

where $A = \frac{M_W^2}{2} + p_x(l)p_x(\nu) + p_y(l)p_y(\nu)$ and $\Delta = E(l)^2 \left(A^2 - \not{E}_{\mathrm{T}}^2 p_T^2(l)\right)$.

The solution which gives the smallest value for $|p_z(\nu)|$ is assumed to be the correct solution and is used to reconstruct the W candidate four-vector. In about 30% of events, a negative value for Δ is found: This comes about because of the finite detector resolution and the presence of "extra" missing energy from, for example, neutrinos from semi-leptonic heavy quark decays or particles which lie outside the detector acceptance. In these events, Δ is set to zero. The invariant mass distribution for the resulting top candidates is shown in Figure 13. As expected, a peak around the nominal top mass ($m_t = 175$ GeV/c^2) is observed, indicating the presence of good top quark candidates. After an optimisation process, it was found that a mass window of $110 < m_t < 220$ GeV/c^2 maximises the statistical significance of the final result and therefore this window is accepted as the definition of a good top candidate from the SM decay channel.

3.2.7 Constraints on the top candidate from the FCNC decay channel

After the products of the SM top decay have been identified, the final step of the analysis process is to combine the Z^0 candidate with good light-quark jet candidates. The combination whose invariant mass lies closest to the nominal top mass is assumed to be the correct one. Parton-level studies have shown that the majority of the $t\bar{t}$ pairs in the signal sample are produced in a "back-to-back" configuration in the transverse plane (the s-channel process being the dominant one). This behaviour can be exploited to reject "fake" top candidates. It is observed that by accepting only candidate events in which the angle between the two top quark candidates satisfies $\cos\phi_{(SMtop,FCNCtop)} < 0$, the background is reduced by 12.5%, compared to only a 3.6% loss in efficiency in the signal sample.

Figure 14 shows the m_{jZ} distribution after the application of all selection requirements. A fit to the distribution using a Breit-Wigner function describes the distribution well, giving a top mass of (175 ± 1) GeV/c^2. This clearly shows that the previously high rate of mis-tagging light-quark jets has been successfully reduced. The final selection requirement is then the use of a window around the nominal top mass of $(150 < m_{jZ} < 200)$ GeV/c^2, which allows the majority of the remaining background to be

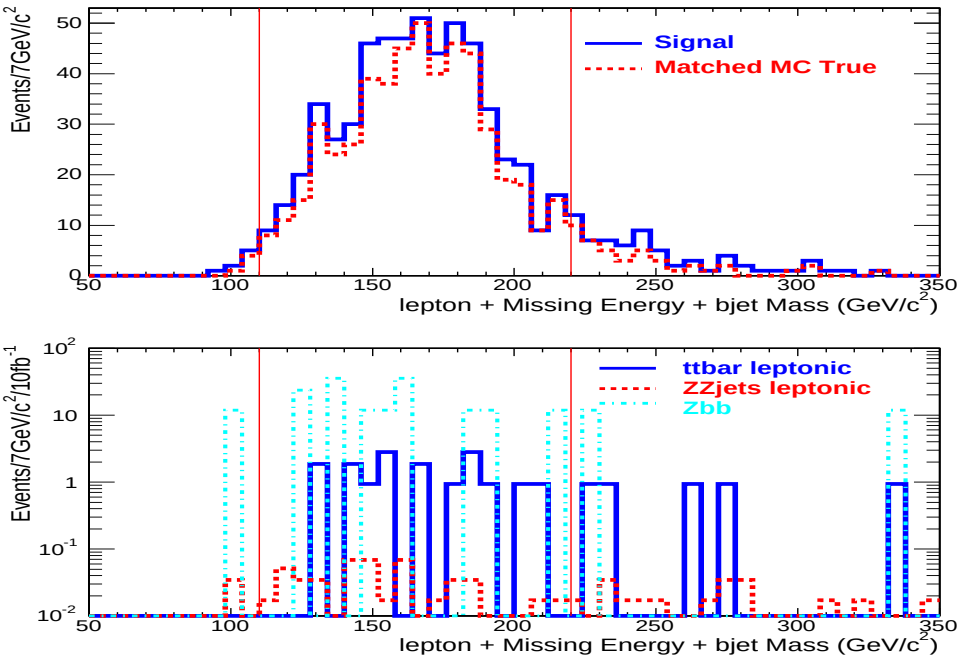

Figure 13: The invariant mass of the e^+/e^- or μ^+/μ^- and missing energy and b-jet combinations for signal and various backgrounds. The lines indicate the mass range ($110 < m_{Wb} < 220$) GeV/c^2 in which candidates are accepted. The background distributions have been normalised assuming an integrated luminosity of L=10 fb^{-1}.

rejected.

The main selection requirements for the $t \to Zq$ channel are summarised briefly below. Each item corresponds to one of the lines in Table. 4; the abbreviations used in Table. 4 are given in parentheses.

- All events must pass the "double electron or double muon" trigger criteria both at Level 1 and in the higher level trigger (*L1 + HLT*);
- Offline, each event must contain either an e^+e^- pair (each satisfying p_T >20 GeV/c) or a $\mu^+\mu^-$ pair (each satisfying $p_T > 10$ GeV/c), whose invariant mass lies within 10 GeV/c^2 of the nominal Z^0 mass. Events with more than one good Z^0 candidate are rejected. (Z^0);
- Each event must also contain a third isolated lepton (either an $e^\pm$ satisfying p_T >20 GeV/c or a $\mu^\pm$ satisfying $p_T > 15$ GeV/c). The combination of this lepton with the missing energy ($\not{E}_T >$ 20 GeV), must have a transverse mass which is less than 120 GeV/c^2. Events with more than one good W candidate are rejected. (W);
- Each event may contain only one jet which is compatible with coming from a b quark (*W + bjet*);
- The invariant mass of the $W^\pm$ and the b-jet should lie in the mass range $(110 < m_{bW} < 220)$ GeV/c^2 (*SM top*);
- Each event must contain at least one jet which is incompatible with coming from a b quark and which satisfies $p_T > 30$ GeV/c. The combination of this with the Z^0 candidate must have an invariant mass in the range $(150 < m_{jZ} < 200)$ GeV/c^2, and must be produced in a "back-to-back" configuration in transverse plane with the b-jet/W candidate combination ($\cos\phi_{(SMtop,FCNCtop)} <0$) (*FCNC top*).

Table. 4 gives the efficiencies for all of these selection requirements in both the signal sample and the different background samples. When no events remain, the upper limit on the efficiency is evaluated assuming it is given by $1/$(number of analysed events).

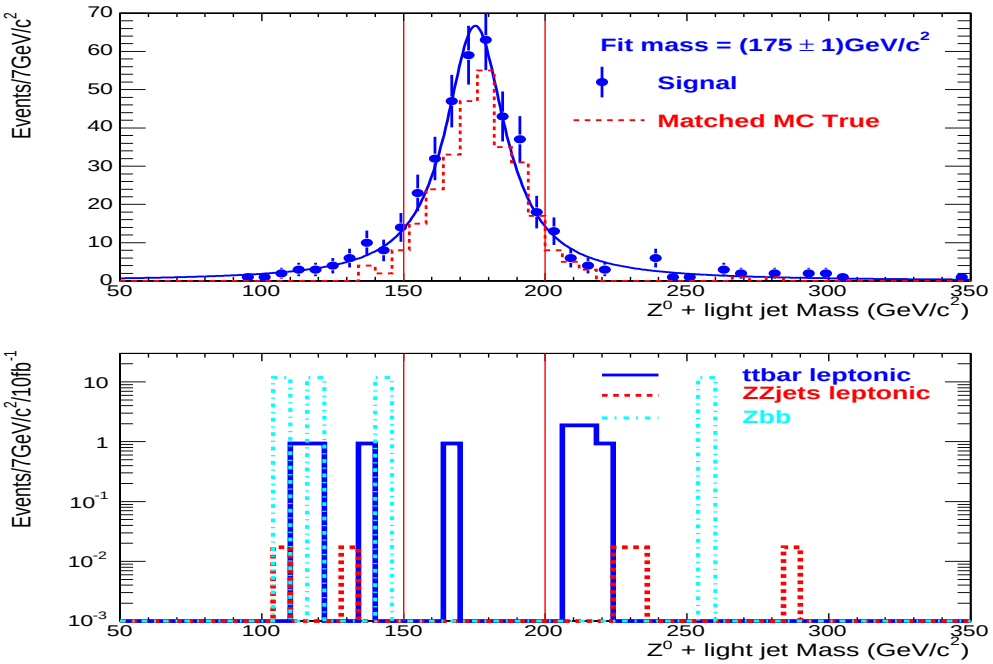

Figure 14: The distribution of the invariant mass of the Z^0/light-quark jet combination in both the signal sample and the different background samples. The lines indicate the mass range ($150 < m_{jZ} < 200$) GeV/c^2 in which candidates are accepted. The background distributions have been normalised assuming an integrated luminosity of L=10 fb^{-1}.

Table 4: The number of events expected to survive the selection requirements described in the text for the $t \to qZ$ channel, assuming an integrated luminosity of 10 fb^{-1}. The effi ciency for each of the selection criteria in both the signal sample and the different background samples is also given (in percentage).

Cut	$t \to Zq$(%)	$t\bar{t}$(%)	ZZ+jets (%)	ZW+jets (%)	WW+jets (%)	Z+jets (%)	Z+ $b\bar{b}$ (%)
$L1 + HLT$	89.10	364.6K (42.90)	946 (59.15)	4207 (16.18)	49.10K (24.80)	2075K (36.01)	2140K (92.26)
Z^0	40.96	12.15K (1.43)	409 (25.57)	1669 (6.42)	1445 (0.73)	809.84K (14.05)	845K (36.45)
W	21.50	47 (0.0055)	106 (6.63)	517 (1.99)	0 (<0.001)	4092 (0.0071)	11.37K (0.19)
$W + bjet$	8.18	22 (0.0026)	1 (0.055)	0 (<0.002)	0 (<0.001)	0 (<0.001)	10.78K (0.18)
$SMtop$	5.59	8 (0.00099)	1 (0.0065)	0 (<0.002)	0 (<0.001)	0 (<0.001)	245 (0.0041)
$FCNCtop$	4.13	1 (0.00011)	0 (<0.0065)	0 (<0.002)	0 (<0.001)	0 (<0.001)	0 (<0.001)

The SM background $t\bar{t} \rightarrow (\nu l b)(\nu l b)$ is the only background that gives a contribution. The total efficiency for the signal selection is $\epsilon_S = 0.041 \pm 0.002$, a total of 1 ± 1 background events accepted for an integrated luminosity of 10 fb^{-1}. The uncertainties reflect the simulated Monte Carlo statistics of the present analysis.

4 The FCNC $t \rightarrow \gamma q$ decay channel analysis

In attempting to identify the FCNC $t \rightarrow \gamma q$ decay channel, similar issues relating to jet-flavour identification must be addressed. In addition, a high-quality single photon selection strategy must be adopted in order to avoid contamination from electrons (which may produce electromagnetic clusters close to photon candidates) or secondary photons within hadronic jets.

4.1 Signal reconstruction procedure

The selection strategy presented here aims first to reconstruct the SM top decay: This is achieved by exploiting the "single electron or muon" triggers both at L1 and in the HLT to identify the lepton from the decay of the W. Once again, efficiencies are high: 96% at L1 and 90% in the HLT. The offline selection of the leptons, missing energy, b-tagged jets and light-quark jets are the same as described for the previous decay channel.

Stricter kinematic cuts are imposed offline for electrons ($p_T > 30$ GeV/c) and muons ($p_T > 20$ GeV/c). More severe thresholds imposed on the missing energy ($\not{E}_{\mathrm{T}}$ >25 GeV) and the light-quark jet transverse momentum (p_T >50 GeV/c) have proven to be very effective in rejecting multi-jet and di-boson backgrounds. The resulting transverse momentum spectra for muons and $\not{E}_{\mathrm{T}}$, along with the jets distribution are shown in Figure 15, Figure 16, Figure 17 and Figure 18. As before, the corresponding distributions for objects matched to the generator-level particles are also shown. As in the $t \rightarrow qZ$ decay channel analysis, the purity of b-tagging is very good after the p_T requirements have been applied, while the expected significant rate of light-quark mis-tagging for all momenta clearly needs to be improved by the imposition of further cuts.

4.1.1 Preselection of photon candidates

Photon selection is performed using a dedicated algorithm [25]. After the candidates have been identified, two further criteria are applied:

- In order to remove Bremsstrahlung photons emitted by charged particles, a minimum distance of $\Delta R > 0.3$ is required between each photon candidate and the electron and muon candidates in the event;
- In order to reject photons radiated within jets, the photon candidate must be isolated. The isolation is performed by summing the p_T of all good tracks ($p_T > 0.9$ GeV/c and number of hits > 4) which lie within a cone of radius $\Delta R = 0.3$ around the electromagnetic cluster. If the sum is less than 1.5% of the transverse energy of the photon candidate, then it is considered to be isolated.

Figure 19 shows the energy distribution of the selected photon candidates. A comparison of this distribution and the corresponding distribution for "matched" photon candidates shows that this selection procedure is effective.

4.1.2 Mass constraints

As for the previous decay channel, the transverse W mass is determined, using Equation 3; the resulting value must be less than 120 GeV/c^2 for the candidate to be accepted. The distribution is shown in

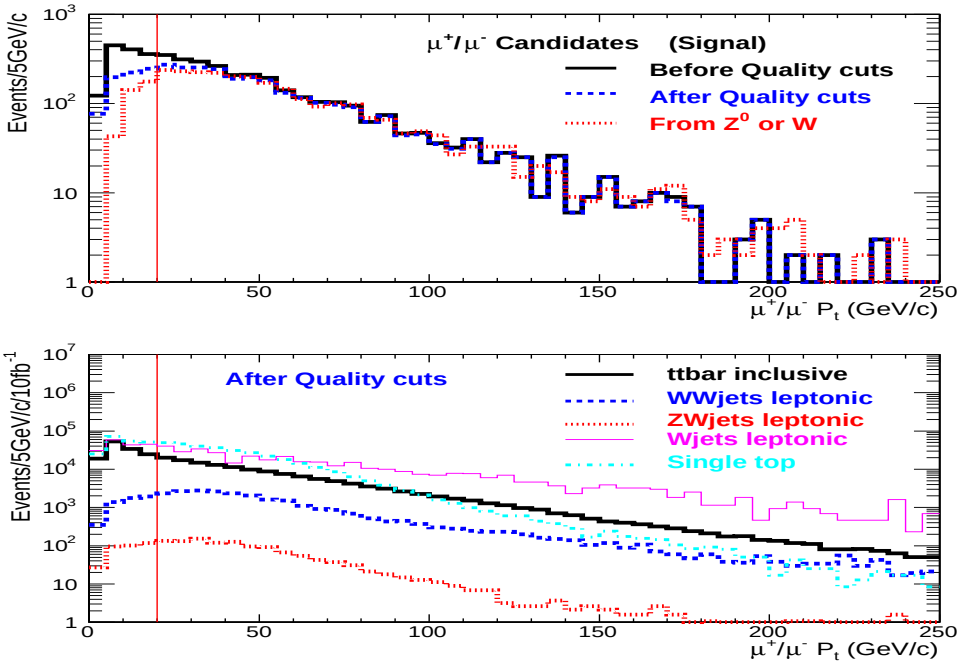

Figure 15: The distribution of the transverse momentum of $\mu^{\pm}$ candidates in both the signal sample and the different background samples. The line indicates the offline selection requirement ($p_T > 20$ GeV/c).The background samples have been normalised, assuming an integrated luminosity of L=10 fb^{-1}.

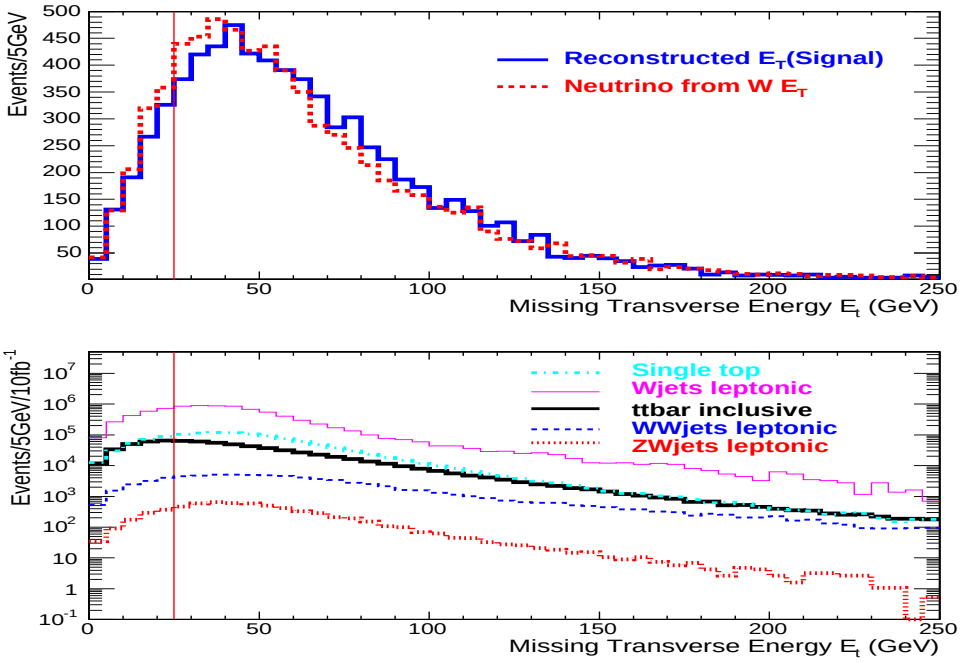

Figure 16: The distribution of the missing transverse energy in both the signal sample and the different background samples. The line indicates the offline selection requirement ($\not\!\!E_T$ >25 GeV).

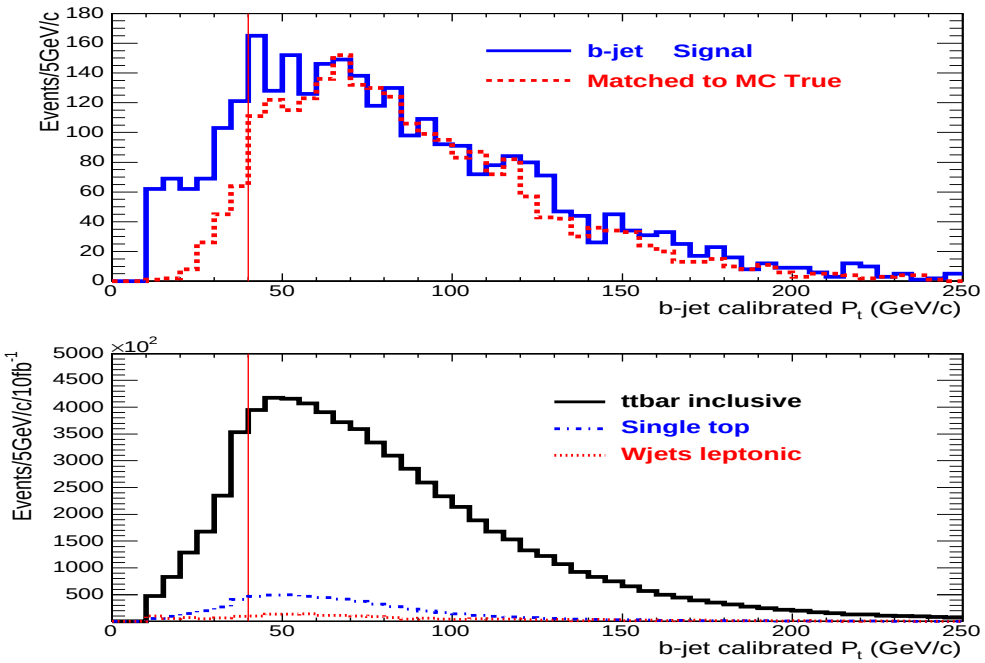

Figure 17: The distribution of the transverse momentum of b-tagged jets in both the signal sample and the different background samples. The line indicates the offline selection cut ($p_T > 40$ GeV/c) and the dotted distribution superimposed on the distribution from the signal sample corresponds to the p_T of the actual b-quark from MC truth information.

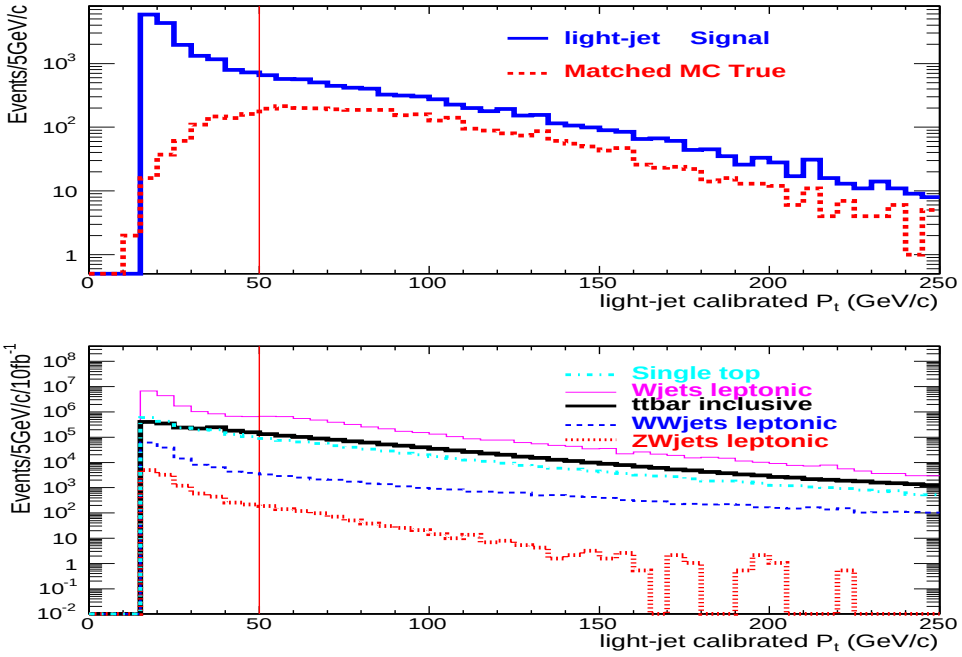

Figure 18: The distribution of the transverse momentum of light-quark jet candidates in both the signal sample and the different background samples. The line indicates the offline selection cut ($p_T > 50$ GeV/c) and the dotted distribution superimposed on the distribution from the signal sample corresponds to the actual u or c quark from MC truth information.

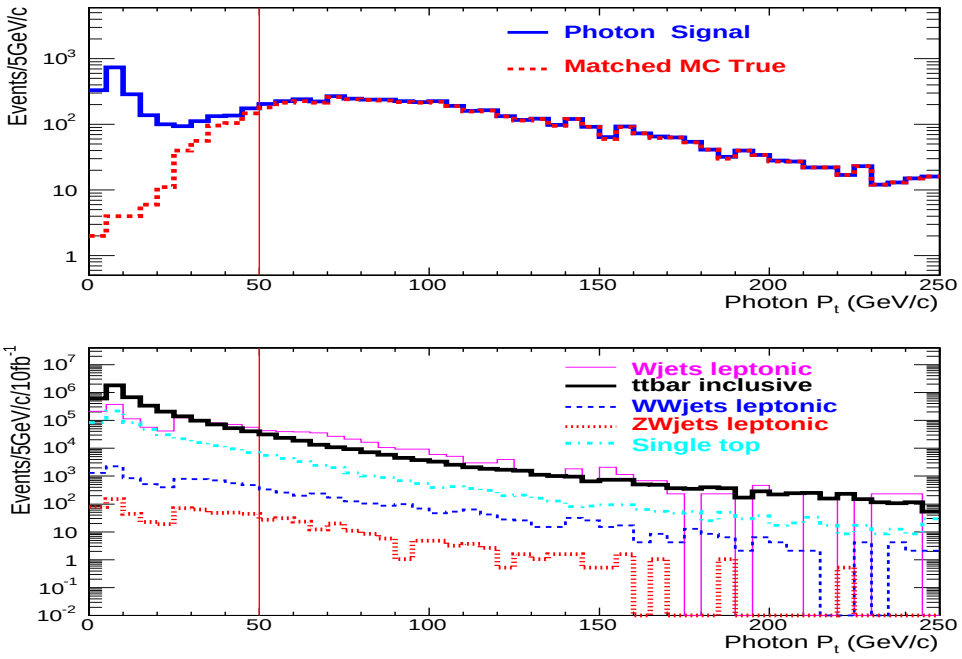

Figure 19: The distribution of the transverse momentum of photon candidates in both the signal sample and the different background samples. The line indicates the offline requirement ($p_T > 50$ GeV/c) and the dotted distribution is corresponding distribution for "matched" photons.

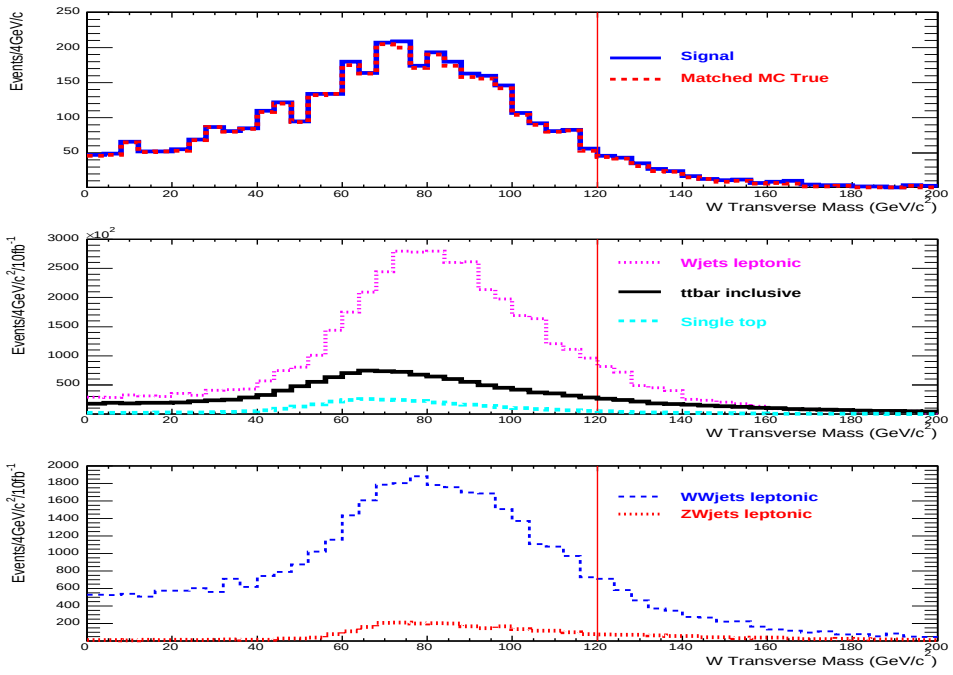

Figure 20: The transverse invariant mass of the $e^{\pm}$ or $\mu^{\pm}$ and missing transverse energy combination in the signal sample and the different background samples. The line indicates the accepted mass region(< 120 GeV/c^2).

Figure 20. It can be seen that, while only a small fraction of the hadronic background is retained, a significant contribution from the di-boson samples is still present.

Only events which contain a good W boson candidate and exactly one b-jet in the final state are considered. Figure 21 shows the top candidate mass distribution for these events; it can be seen that only the SM $t\bar{t}$, Single top and W plus jets background samples survive after these requirements.

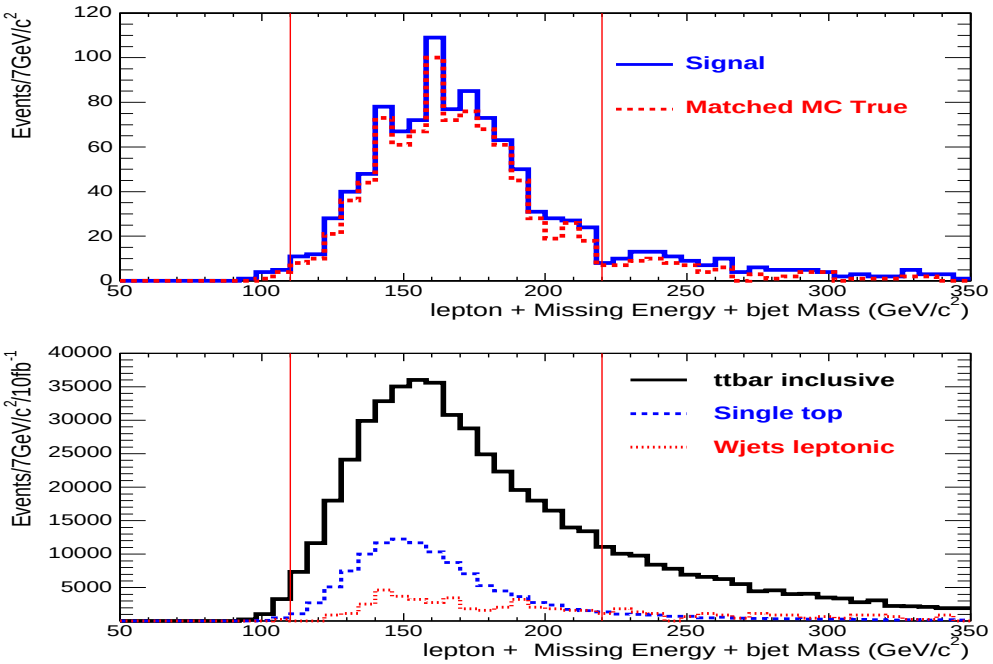

Figure 21: The invariant mass of the $e^{\pm}/\mu^{\pm}$, missing energy and b-jet combinations in the signal sample and the different background samples. The lines indicate the accepted mass range ($110 < m_{bW} < 220$) GeV/c^2. The background samples are normalised assuming an integrated luminosity of L=10 fb^{-1}.

Only events containing a SM top quark candidate whose mass satisfies ($110 < m_{bW} < 220$) GeV/c^2 and a good photon candidate are retained for further analysis. Once again the angle in transverse plane between the two top quarks candidates is exploited to reduce background contributions; figure 22 shows the distribution of $\cos\phi_{(SMtop,FCNCtop)}$ for this sample. A requirement of $\cos\phi_{(SMtop,FCNCtop)} < -0.95$ is very effective at rejecting all sources of background, except for that coming from SM $t\bar{t}$ production and single top production.

Figure 23 shows the $m_{j\gamma}$ distribution after all cuts have been applied. A fit using a Breit-Wigner function describes the distribution well and gives a top mass of (178 ± 1)GeV/c^2. The final selection requirement is then the use of a window around the nominal top mass of ($150 < m_{j\gamma} < 200$) GeV/c^2, which allows the majority of the remaining background to be rejected.

A brief summary of the main selection requirements for the $t \to \gamma q$ channel is given below. Each item corresponds to a line in Table. 5; the abbreviations used in Table. 5 are given in parentheses.

- All events must pass the "single electron or muon" trigger criteria at L1 and in the HLT (*L1 + HLT*);
- Offline, each event must contain either an $e^{\pm}$ (with p_T >30 GeV/c) or a $\mu^{\pm}$ (with p_T > 20 GeV/c) and more than 25 GeV of missing transverse energy. The combination of the lepton candidate and the missing transverse energy must have a transverse invariant mass which satisfies $M_T < 120$ GeV/c^2. Events with more than one good W candidate are rejected. (W);
- Each event must contain exactly one jet (with p_T >40 GeV/c) which is compatible with coming

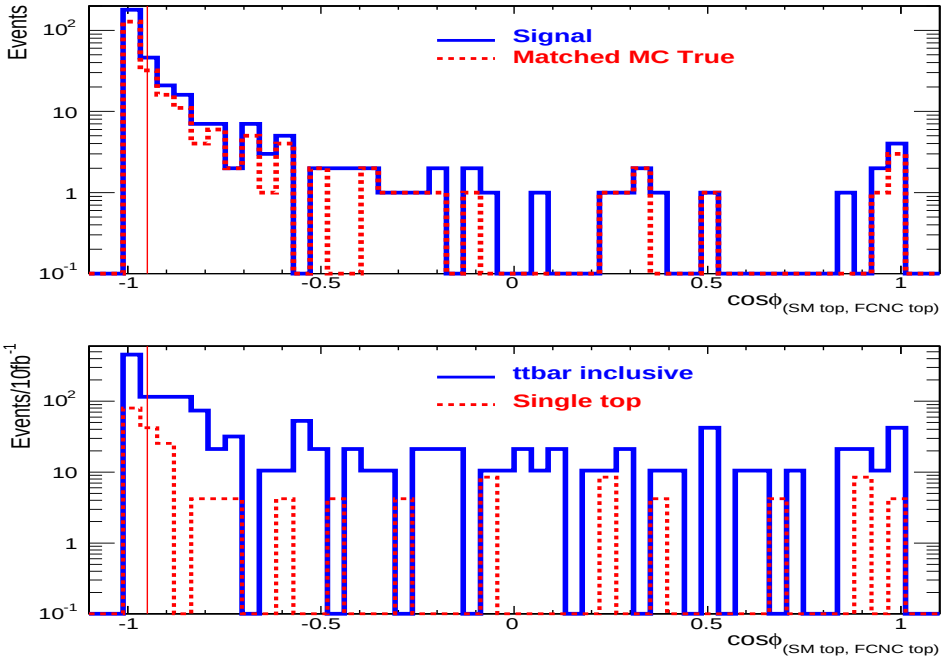

Figure 22: The distribution of the cosine of the angle between the two reconstructed top quark candidates in the transverse plane. A cut of $\cos\phi_{(SMtop,FCNCtop)}$ <-0.95 is very effective for reducing the contribution from all sources of background.

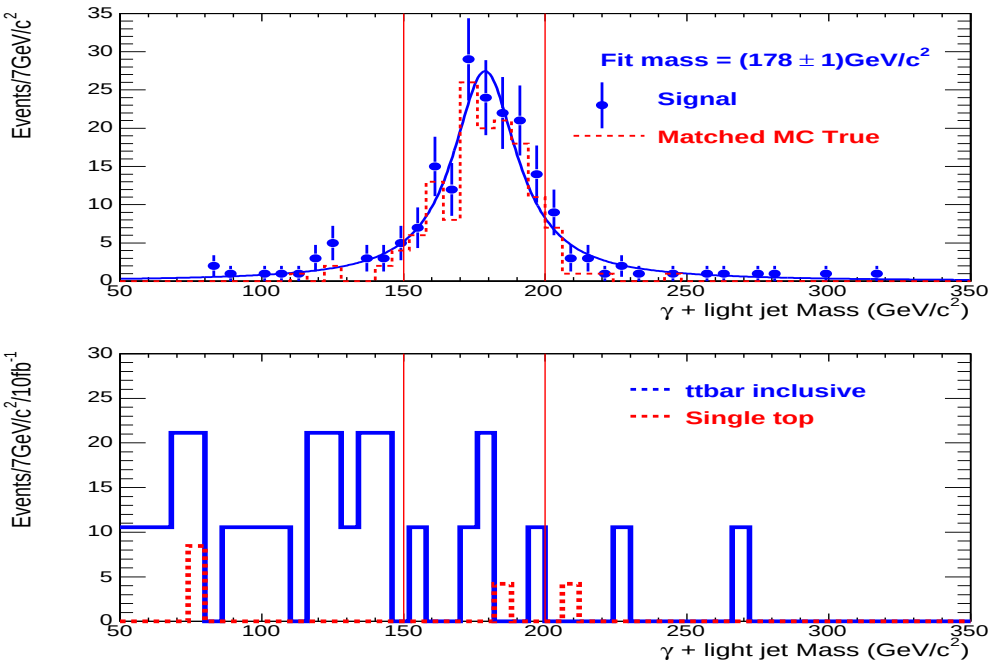

Figure 23: The invariant mass distribution of the γ/light-quark jet combination in the signal sample and the different background samples. The lines indicate the accepted mass region $(150 < m_{j\gamma} < 200)$ GeV/c^2. The background samples are normalised assuming an integrated luminosity of L=10 fb^{-1}.

Table 5: The number of events expected to survive the selection requirements described in the text for the $t \to q\gamma$ channel, assuming an integrated luminosity of 10 fb^{-1}. The effi ciency for each of the selection criteria in both the signal sample and the different background samples is also given (in percentage).

Cut	$t \to \gamma q$ (%)	$t\bar{t}$ *incl.* (%)	ZW+jets (%)	WW+jets (%)	W+jets (%)	W+$b\bar{b}$ (%)	*single-top t ch.*
$L1 + HLT$	90.2	3,249K (39.0)	6630 (25.5)	81.38K (41.1)	8.691M (20.2)	*not avail.*	*not avail.*
W	42.6	1,283K (15.4)	2600 (10.0)	32.48K (16.4)	3.829M (8.9)	55.80K (18.6)	210.9K (26.0)
$SMtop$	11.4	424.9K (5.1)	3 (0.01)	198 (0.1)	38.72K (0.09)	2430 (0.81)	70.40K (8.67)
$FCNCtop$	2.1	52 (0.00063)	0 (<0.002)	0 (<0.001)	0 (<0.0005)	0 (<0.001)	2 (0.00025)

from a b quark and which, in combination with the W candidate, has an invariant mass in the range ($110 < m_{bW} < 220$) GeV/c^2 (*SM top*);

- Each event must contain exactly one isolated photon which satisfies p_T >50 GeV/c and one jet which is imcompatible with coming from a b-quark and which satisfies $p_T > 50$ GeV/c. The top candidate which is reconstructed from these two objects must be in a "back-to-back" configuration in the tranverse plane with the other top quark candidate ($\cos\phi_{(SMtop,FCNCtop)} < -0.95$) and have an invariant mass in the range ($150 < m_{j\gamma} < 200$) GeV/c^2 (*FCNC top*).

Table. 5 gives the efficiencies for all the different selection requirements, both for the signal sample and for the different background samples. When no events remain, the upper limit on the efficiency is evaluated assuming it is given by $1/$(number of analysed events). The background contributions from W production in association with a $b\bar{b}$ and single top production have been processed with the fast simulation and hence, no trigger information is available. The contribution from the single top production background sample is much smaller than that from the dominant SM $t\bar{t}$ background sample; this means that the assumptions made for the $t \to qZ$ channel also hold here.

4.1.3 Analysis of the multi-jet background sample

The QCD background studied in these analyses deserves special treatment, as the analysed MC sample is several orders of magnitude smaller than the expected number of events (as shown in Tab. 3). Indeed, a strategy has to be devised in order to reliably extract a rejection factor for these background processes and to verify whether it is possible for some events to pass all the selection requirements. To accomplish this task, the full procedure is separated out into a set of uncorrelated selection requirements and the absolute efficiency for each of them is then computed. The rejection factor for the global selection will then be the product of the efficiencies for each independent requirement. The selection requirements for which efficiencies have been separately evaluated are given below. The labels used in Table. 6 are given in parentheses.

1. Each event should contain two jets with $p_T > 40$ GeV/c, without the application of b-tagging techniques and a missing transverse energy which satisfies $\not{E}_{\rm T} > 25$ GeV/c (*2 hard jets*);

2. Each event should contain an isolated photon which satisfies $p_T > 50$ GeV/c. This selection requirement could, in fact, be anti-correlated with the item 1 above because the jet could be identified as the photon and vice versa. The assumption that they are actually uncorrelated must therefore be considered to be strongly conservative (*hard* γ);

3. Each event should contain a good lepton candidate. Of course, the real lepton from the W decay will be directly correlated with the missing energy from the neutrino; however, it has been observed that the majority of the reconstructed leptons in the multi-jet background samples are actually

Table 6: The absolute effi ciencies for the four independent selection requirements described in the text. The values are quoted both for the multi-jet QCD background sample and the SM $t\bar{t}$ sample. The last two columns contain the combined rejection factor and the number of expected events from a dataset with an integrated luminosity of 10 fb^{-1}.

Cut	*2 hard jets*	*hard* γ	*hard lepton*	*b-tag*	*Total Eff.*	*Expected evs.*
QCD (50$<\hat{p}_T<$80)GeV/c	0.2%	0.04%	0.07%	0.5%	2.8×10^{-11}	0.6
QCD (80$<\hat{p}_T<$120)GeV/c	1.0%	0.2%	0.2%	0.5%	2.0×10^{-10}	6.1
QCD (120$<\hat{p}_T<$170)GeV/c	3.4%	0.3%	0.3%	0.5%	1.5×10^{-9}	7.4
QCD (170$<\hat{p}_T<$230)GeV/c	8.5%	0.6%	0.6%	0.5%	1.5×10^{-8}	15.1
QCD (230$<\hat{p}_T<$300)GeV/c	14%	0.6%	0.6%	0.5%	2.5×10^{-8}	6.1
QCD (300$<\hat{p}_T<$380)GeV/c	20%	0.7%	1%	0.5%	7×10^{-8}	4.3
QCD (380$<\hat{p}_T<$470)GeV/c	23%	0.6%	1%	0.5%	6.9×10^{-8}	1.2
QCD (470$<\hat{p}_T<$600)GeV/c	24%	0.5%	1.2%	0.5%	7.2×10^{-8}	0.5
QCD (600$<\hat{p}_T<$800)GeV/c	25%	0.5%	1.6%	0.5%	1.5×10^{-7}	0.2
QCD (800$<\hat{p}_T<$1000)GeV/c	25%	0.4%	2%	0.5%	1×10^{-7}	0.3
$t\bar{t}$ *inclusive*	35%	0.8%	30%	30%	2.5×10^{-4}	2083

mis-identified hadrons. It is therefore a reasonable assumption that this selection requirement is uncorrelated with the item 1 above (*hard lepton*);

The b-tagging requirements are not applied to the surviving sample, in order to retain events for further study. Under the reasonable assumption that the vast majority of jets in this background sample will not have been produced by b-quarks, the events which suriving the b-tagging procedure should be predominantly mis-tagged light-quark jets. In this case, the mis-tagging efficiency given in Section. 3.2.3 can be used as the uncorrelated efficiency for this selection requirement (labelled as *b-tag*) in Table. 6. The efficiencies for these uncorrelated selection requirements are given in Table. 6, along with the overall combined efficiency and the number of expected events.

The overall effect of these selection requirements is to reduce the very large multi-jet QCD background contribution to approximately 42 events, assuming an integrated luminosity of 10 fb^{-1}. The surviving events occur mainly in the range ($100 < \hat{p}_T < 500$) GeV/c. It is possible to argue that these events will fail the mass constraints placed on the W and top candidates and therefore the contribution from this source of background may well be significantly smaller.

This additional reduction factor from applying mass constraints can be estimated using the SM $t\bar{t}$ sample, as this has higher remaining statistics after the application of the uncorrelated selection requirements than the multi-jet sample. As there will clearly be a correlation between the missing energy requirement and the lepton selection in this case, only a lower limit on the final efficiency can be estimated. The effect of the b-tagging procedure is assumed to be that given in Sec. 3.2.3. A comparison of the results for the $t\bar{t}$ background sample given in Table. 6 and the number of $t\bar{t}$ events that remain in the full analysis implies that the final mass constraints and the cos$\phi_{(SMtop,FCNCtop)}$ requirement have a rejection power better than 2.5%. Assuming that this is also true for the multi-jet QCD background sample (a rather pessimistic hypothesis), then this suggests that only one event will remain after the application of all cuts. It is therefore reasonable to neglect the multi-jet QCD sample as a source of background for this analysis.

The only sources of background for this analysis are therefore SM $t\bar{t}$ and single top (s-channel) production. The total efficiency for signal selection is $\epsilon_S = 0.021 \pm 0.002$, with an expected 54.0 ± 7.3 background events surviving the selection process for an integrated luminosity of 10 fb^{-1}. The uncertainties reflect the simulated Monte Carlo statistics of the present analysis.

Table 7: The results from the branching ratio estimation for the two FCNC decay channels. The minimum number of expected signal events is given assuming a 5-sigma discovery.

channel	S	$BR(\times 10^{-4})$
$t \to Zq$	11.2	11.4
$t \to \gamma q$	43.0	5.7

5 Sensitivity estimation

In order to estimate the sensitivity of the CMS experiment to FCNC decays in the top sector, it is assumed that an observation of new physics will only be claimed when the signal significance is at least 5. When the number of background events (B) is small compared to the number of signal events (S), the most appropriate definition of significance is [30]:

$$S_{c12} = 2\left(\sqrt{B+S} - \sqrt{B}\right), \tag{4}$$

where S_{c12} represents the probability (in number of standard deviations) that an expected number of background events fluctuates above the observed number of events $S + B$ with Poisson statistics. Equation 4 can be used to evaluate the minimum number of signal events which would constitute a discovery of FCNC decays for a given level of significance. Equally, the number of signal events for the $t \to Zq$ and $t \to \gamma q$ decay channels can be expressed as:

$$S(t \to Zq) = 2 \times BR(t \to Zq) \times Br\,(W \to l\nu) \times Br\,(Z \to ll) \times \sigma(t\bar{t}) \times L \times \epsilon_S(t \to Zq)$$
$$S(t \to \gamma q) = 2 \times BR(t \to \gamma q) \times Br\,(W \to l\nu) \times \sigma(t\bar{t}) \times L \times \epsilon_S(t \to \gamma q)$$

respectively, where L = 10 fb^{-1}, $\sigma(t\bar{t})$ = 833 pb, $BR(W \to l\nu)$ = 0.2136, $BR(Z \to ll)$ = 0.0673 ($l = e, \mu$) and ϵ_S is the selection efficiency. From these formulae, the values for $BR(t \to Zq)$ and $BR(t \to \gamma q)$ can be calculated for any significance level S_{c12}.

Without the inclusion of systematic effects, the sensitivity can be estimated simply from the results given in Sections 3 and 4. Figure 24 shows the sensitivity to FCNC decays as a function of the significance level: For $S_{c12} = 5$, it can be seen that $BR(t \to Zq) = 11.4 \times 10^{-4}$ and $BR(t \to \gamma q) = 5.7 \times 10^{-4}$.

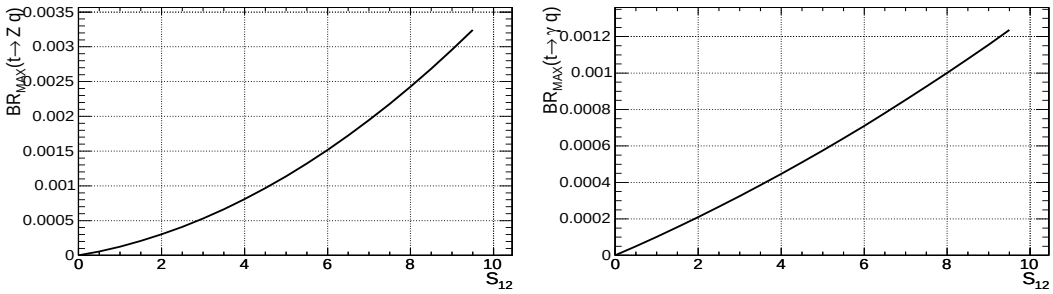

Figure 24: The branching ratios of FCNC decays versus the signal signifi cance for $t \to Zq$ (left) and $t \to \gamma q$ (right) assuming a dataset with an integrated luminosity of 10 fb^{-1}. The estimated upper limits for the branching ratios for $S_{c12} = 5$ are $BR(t \to Zq) = 11.4 \times 10^{-4}$ and $BR(t \to \gamma q) = 5.7 \times 10^{-4}$. Effects of systematic uncertainties have not been included.

These estimates represent the smallest possible observable branching ratios for FCNC decays. In the 10 fb^{-1} scenario, they correspond to a minimum number of expected observable events of 11.2 (for the $t \to Zq$ decay channel) and 43.0 (for the $t \to \gamma q$ decay channel), as reported in Tab. 7.

5.1 The impact of systematic uncertainties

The results presented in the previous section will be altered by sources of systematic uncertainties. These sources can be divided into two groups: those related to theoretical issues and those related to detector issues. The procedures for dealing with these two groups follow those described in [26] and [27]. The majority of the sources of systematic uncertainties considered are important for both decay channels, thus they are discussed together.

5.1.1 Systematic effects related to the detector

The impact of these systematic uncertainties is estimated by shifting or rescaling the properties of the leptons, jets or photons after reconstruction, so that their effect on the selection efficiency and the suriving number of background events may be evaluated. Only uncorrelated systematic effects are considered; a list is given below.

Lepton Energy Scale (LES): Imperfect knowledge of the inactive material, magnetic field and detector alignment will induce an uncertainty in the reconstructed lepton 4-momentum. In addition, reconstruction of the electron energy will be limited by the energy resolution of the calorimeters, making this source of systematic uncertainty much more important for electron/photons than for muons. It is accounted for by varying the reconstructed energy and momentum by ± 0.005. The same procedure is applied for the photon energy scale uncertainty, while for the muons it is assumed to be negligible. Both analyses prove to be sensitive to the lepton energy scale as the background is increased in both cases;

Jet and Missing Energy Scale (JES+MES): The jet energy scale uncertainty (after an integrated luminosity of 10 fb^{-1}) is expected to be $\pm 5\%$ for jets with p_T =20 GeV/c and $\pm 2.5\%$ for jets with $p_T > 50$ GeV/c. Inbetween a linear dependence is assumed. As the missing energy is determined from jet information, the missing energy scale will be fully correlated with the jet energy scale and therefore has to be changed simultaneously by $\pm 5\%$;

b-tagging uncertainty: The b-tagging uncertainty is assumed to be 4% after an integrated luminosity of 10 fb^{-1} [28]. Mistagging of a light-quark jet as a b-jet can be reproduced by assuming a non-b-tagged jet is actually a b-tagged jet 4% of the time. As the present analyses exploit anti-b-tagging to reduce the SM $t\bar{t}$ background, anti-tagging a b-jet instead of a non-b-jet is simulated by assuming a b-tagged jet to be a non-b-tagged jet approximately 4% of the time. It is found that the tagging uncertainty does not heavily dependent from the p_T and η of the jets.

As these analyses do not require precise mass or energy measurements, limited resolution for the lepton and jet energy scales, as well as shifts in the mass distribution are not important and therefore were not taken into account.

5.1.2 Theoretical Uncertainties

The spectrum of theoretical uncertainties considered in these analyses is given below:

- The uncertainty on the $t\bar{t}$ NLO cross-section predictions results in a variation in the number of background events. The errors quoted for the prediction given in Eq. 1 come from scale uncertainties ($\sim 5\%$) and from the PDF uncertainties ($\sim 2.5\%$, [4]): adding these two terms in quadrature, a value of 5.6% is obtained. The selection efficiencies will not be affected by this uncertainty;
- the statistical uncertainty arising from the size of the Monte Carlo datasets will produce fluctuations in the expected number of background events, which must be considered as a source of systematic uncertainty;

Table 8: Effects of the different sources of systematic uncertainty on the FCNC branching ratios. The last row indicates the lowest observable 5-sigma FCNC branching ratios for an integrated luminosity of 10 fb^{-1}, including all sources of systematic uncertainty.

	$t \to Zq$ ($\times 10^{-4}$)	$t \to \gamma q$ ($\times 10^{-4}$)
$BR(stat)$	11.4	5.7
jet energy scale	+0.4	+0.6
b jet mistagging	+0.2	+1.8
light jet antitagging	+0.5	+0.9
lepton energy scale	+2.4	+0.5
$\sigma(t\bar{t})$	+0.1	+0.5
MC statistics in B	+2.4	+1.3
MC statistics in S	+0.7	+0.5
Luminosity	+0.1	+0.5
$BR(total)$	14.9	8.4

- similarly, the statistical power of the analysis is linked to the available number of signal events. Consequently, any fluctuation of the efficiency must also be considered a source of systematic uncertainty.

Finally, the uncertainty on $t\bar{t}$ production from the machine itself has to be regarded as a systematic effect. In the low luminosity phase, the uncertainty on the instantaneous luminosity is expected to be 5% [29].

5.2 Sensitivity estimation including systematic uncertainties

As a final step in the analysis, fluctuations of both B and ϵ_S have to be taken into account when evaluating the branching ratios. The contributions can be included by convoluting a Poissonian distribution with the background distribution, which is commonly considered to be Gaussian if only detector effects are taken into account. The contributions from theoretical uncertainties in the background are assumed to be a fixed percentage. The determination of S_{c12} in this case has been performed using a package designed to take into account all these points [31]. By adopting this tool, the smallest number of signal events required for an observation is evaluated for each systematic source, then combined with the resulting ϵ_S to obtain the branching ratio. The impact of each individual source of systematic uncertainty is given in Table. 8.

Experimental sources of systematic uncertainty, such as the control of the lepton energy scale or the b-tagging procedure are expected to be the most significant. The statistical uncertainty on the expected number of background events makes a large contribution to the global systematic uncertainty. Refined techniques for background estimation will reduce this uncertainty once data is available.

All sources of systematic uncertainty considered here are assumed to be uncorrelated, apart from the theoretical uncertainties. Including all these effects, the minimum detectable FCNC branching ratios for a 5-sigma sensitivity and at integrated luminosity of 10 fb^{-1} are $BR(t \to Zq) = 14.9 \times 10^{-4}$ and $BR(t \to \gamma q) = 8.4 \times 10^{-4}$.

6 Conclusions and outlook

In order to evaluate the CMS discovery potential for FCNC top decays, the $t \to Zq$ and $t \to \gamma q$ decay channels have been studied for a dataset corresponding to an integrated luminosity of L = 10 fb^{-1} using Monte Carlo data which has been processed using the full detector simulation. A cut-based analysis has

been defined, using objects reconstructed using the software packages developed by the CMS Collaboration. In particular, the selection procedure includes an extensive set of quality requirements on the final state lepton candidates and is heavily reliant on good b-tagging capabilities. This procedure has been shown to be very effective in reducing the large background contributions from Standard Model $t\bar{t}$, QCD multi-jet and Z^0 production in associated with a $b\bar{b}$ pair, while retaining a reasonable selection efficiency and minimising the impact of systematic uncertainties. An upper limit of 11.4×10^{-4} has been determined for the $t \to Zq$ decay channel and 5.7×10^{-4} for the $t \to \gamma q$ decay channel.

It is interesting to note that some improvements to these results will come about "automatically", for example, the b-tagging procedure will improve with increasing integrated luminosity, while the increase in instantaneous luminosity will decrease the discovery limits for both these decay channels. Assuming that the selection efficiency is unaffected by moderate luminosity improvements (that is, assuming that increased pile-up does not change the ability to identify the key hard objects in the final states of both decay channels), the effect of the increase in integrated luminosity on the branching ratio results can be evaluated very simply. Figure 25 shows the branching ratio as a function of the luminosity for both decay channels, based on the numbers presented in this paper, with(solid) and without(dashed) the inclusion of systematic uncertainties. From the curves in Figure 25, it can be expected that an improvement in the upper limit on the branching ratios by a factor of 2 will be possible for a five-fold increase in integrated luminosity.

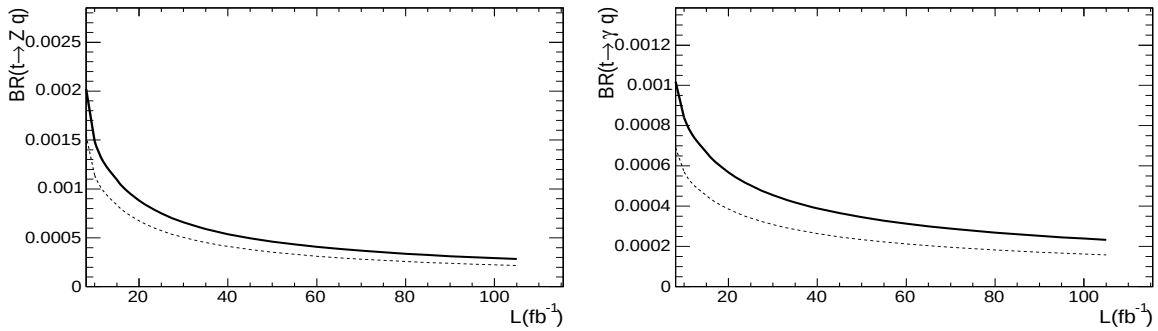

Figure 25: The branching ratios of FCNC top decays as a function of integrated luminosity, for $t \to qZ$ (left) and $t \to q\gamma$ (right), assuming a 5-sigma discovery level. These curves are based on the values given in the text, which correspond to an integrated luminosity of L=10 fb^{-1}. The two curves represent the branching ratios including (solid line) and excluding (dashed line) the contribution from systematic uncertainties.

It is important to note that this would improve the current experimental limits for FCNC top decays by almost two orders of magnitude for the $t \to Zq$ decay channel and by one order of magnitude for the $t \to \gamma q$ decay channel, allowing models of new physics scenarios to be tested.

Aknowledgements

The authors would like to thank Jo Cole and Salvatore Mele for their very valuable comments in refereeing this note. We are strongly indebted to Roberto Tenchini for his support and important suggestions, and to Guido Tonelli and Sergey Slabospitsky who put their wide experience at our disposal. A special mention is needed for Roberto Dell'Orso and Athanasios Markou who made it possible for the Athens and Pisa groups to meet together: the authors' hope is that in developing the work, this collaboration will become more and more effective. We also would like to thank the CMS production team for providing the Monte Carlo samples, all the members of CMS who contributed to the development of all software packages used in this study and our home institutes that provided the financial support. The Greek co-authors aknowledge financial support from the Greek Secrerariat of Research and Techology.

References

[1] CDF Collaboration, Phys. Rev. Lett. **74**, 2626 (1995); D0 Collaboration, Phys. Rev. Lett. **74**, 2632 (1995)

[2] P. Nason, S. Dawson, R. K. Ellis, Nucl. Phys. B **303**, 607 (1988)

[3] D. Chakraborty, J. Konigsberg, D. Rainwater, Ann. Rev. Nucl. Part. Sci. **53**, 301 (2003)

[4] M. Mangano, private communication

[5] G. Eilam, J. L. Hewett and A. Soni, Phys. Rev. D **44**, 1473 (1991); B. Mele, S. Petrarca, A. Soddu, Phys. Lett. B **435**, 401 (1998)

[6] C.-H. Chang, X.-Q. Li, J.-X. Wang, M.-Z. Yang, Phys. Lett. B **313**, 389 (1993) C.-S. Huang, X.-H. Wu and S.-H. Zhu, Phys. Lett. B **452**, 143 (1999)

[7] H. E. Haber and G. L. Kane, Phys. Rept. **117**, 75 (1985)

[8] C. S. Li, R. J. Oakes and J. M. Yang, Phys. Rev. D **49**, 293 (1994); G. Couture, C. Hamzaoui and H. Konig, Phys. Rev. D **52**, 1713 (1995); J. L. Lopez, D. V.Nanopoulos and R. Rangarajan, Phys. Rev. D **56**, 3100 (1997); G. M. de Divitiis, R. Petronzio and L. Silvestrini, Nucl. Phys. B **504**, 45 (1997)

[9] J. M. Yang and C. S. Li, Phys. Rev. D **49**, 3412 (1994); J. Guasch and J. Sola, Nucl. Phys. B 562, 3 (1999); G. Eilam, A. Gemintern, T. Han, J.M. Yang, X. Zhang, Phys. Lett. B **510**, 227 (2001)

[10] C. S. Li, X. Zhang and S. H. Zhu, Phys. Rev. D **60**, 077702 (1999)

[11] J. L. Diaz-Cruz *et al.*, Phys. Rev. D **41**, 891 (1990); G. Eilam, J. L. Hewett and A. Soni, Phys. Rev. D **44**, 1473 (1991); X.L. Wang *et al.*, Phys. Rev. D **50**, 5781 (1994); D. Atwood, L. Reina and A. Soni, Phys. Rev. D **53**, 1199 (1996); S. Bar-Shalom, *et al.*, Phys. Rev. Lett. *79*, 1217(1997); W. S. Hou, G.-L. Lin and C.-Y. Ma, Phys. Rev. D **56**, 7434(1997); S. Bejar, J. Guasch and J. Sola, Nucl. Phys. B 675, 270 (2003); T. Han and J. Hewett, Phys. Rev. D **60**, 074015 (1999); F. del Aguila, J. A. Aguilar-Saavedra, R. Miquel, Phys. Rev. Lett. **82**, 1628 (1999)

[12] S. Chekanov *et al.* (ZEUS Collaboration), Phys. Lett. B **559**, 153 (2003)

[13] G. Abbiendi *et al.* (OPAL Collaboration), Phys. Lett. B **521**, 181 (2001)

[14] Y. P. Gouz and S. R. Slabospitsky, Phys. Lett. B **457**, 177 (1999)

[15] S. R. Slabospitsky, L. Sonnenschein, Comput. Phys. Commun. **87**, 148 (2002)

[16] T. Sjöstrand and M. Bengtsson, Comput. Phys. Commun. **43**, 367 (1987); T. Sjostrand, Comput. Phys. Commun. **82**, 74 (1994)

[17] CMS Collaboration, *Object oriented Simulation for CMS Analysis and Reconstruction*, Physics TDR Vol.I, Chapter 2; http://cmsdoc.cern.ch/OSCAR/

[18] CMS Collaboration, *Object-oriented Reconstruction for CMS Analysis*, Physics TDR Vol.I, Chapter 2; http://cmsdoc.cern.ch/ORCA/

[19] CMS Collaboration, *FAMOS, FAst MOnte-Carlo Simulation*, Physics TDR Vol.I, Chapter 2; http://cmsdoc.cern.ch/FAMOS/

[20] CERN/LHCC/2006-01, CMS Physics TDR Vol.I, February 2006, Sec 3.4; CERN/LHCC/2002-26, CMS DAQ and HLT TDR 6.2, December 2002; http://cmsdoc.cern.ch/cms/TDR/DAQ/daq.html

[21] CERN/LHCC/2006-01, CMS Physics TDR Vol.I, February 2006, Sec 10.4.7

[22] CERN/LHCC/2006-01, CMS Physics TDR Vol.I, February 2006, Sec 11.2.1

[23] CERN/LHCC/2006-01, CMS Physics TDR Vol.I, February 2006, Sec 11.6.3

[24] CERN/LHCC/2006-01, CMS Physics TDR Vol.I, February 2006, Sec 12.2.2

[25] CERN/LHCC/2006-01, CMS Physics TDR Vol.I, February 2006, Sec 10.3

[26] P. Bartalini, R. Chierici, A. De Roeck, *Guidelines for the Estimation of Theoretical Uncertainties at the LHC*, CMS NOTE-2005/013

[27] http://cmsdoc.cern.ch/cms/PRS/gentools/www/systematics/syserr.html

[28] S. Lowette, J. D'Hondt, J. Heyninck, *Offline Calibration of b-Jet Identification Efficiencies*, CMS NOTE 2006/013

[29] V. A. Khoze, A. D. Martin, R. Orava, M. G. Ryskin, Eur.Phys.J.**C 19**,313 (2001)

[30] V. Bartsch, G. Quast, *Expected signal observability at future experiments*, CMS NOTE-2005/004

[31] http://cmsdoc.cern.ch/˜bityukov